NATIONAL AERONAUTICS AND SPACE ADMINISTRATION

Technical Memorandum 33-637

Interplanetary Charged Particle Environments

T. N. Divine

JET PROPULSION LABORATORY
CALIFORNIA INSTITUTE OF TECHNOLOGY
PASADENA, CALIFORNIA

August 1, 1973

NATIONAL AERONAUTICS AND SPACE ADMINISTRATION

Technical Memorandum 33-637

Interplanetary Charged Particle Environments

T. N. Divine

JET PROPULSION LABORATORY
CALIFORNIA INSTITUTE OF TECHNOLOGY
PASADENA, CALIFORNIA

August 1, 1973

PREFACE

The work described in this report was performed by the Project Engineering Division of the Jet Propulsion Laboratory.

CONTENTS

ABSTRACT

Current state-of-the-art knowledge of the solar wind, solar particle events, and galactic cosmic rays is reviewed for the development of space vehicle design criteria based on these interplanetary environments. These criteria are described quantitatively in terms of intensity, flux and fluence, and their dependences on time, position and energy, and the associated probabilities and related parameters, for electrons, protons and other ions.

1. INTRODUCTION

The design of space vehicles for operation in interplanetary space requires both qualitative and quantitative descriptions of charged particle environments. These environments comprise the solar wind, solar particle events, and galactic cosmic rays, for all of which extensive data have been reported in the literature. The state-of-the-art review and the resulting design criteria which are developed in the following sections are based primarily on results of experiments aboard interplanetary and high-altitude earth-orbiting spacecraft published through 1972.

Solar cells are particularly sensitive to charged particle impact, and important degradation in their power output has been traced to the effect of prolonged exposure to the solar wind. Degradation of other spacecraft surfaces, particularly coatings and lenses, sometimes occurs for long residence times in interplanetary space, requiring serious design consideration for all these environments. Interference, including detector saturation, spurious experiment and system operations signals and responses, occasionally results from energetic proton impact in severe solar particle events. Galactic cosmic ray impact can lead to interference and failure in sensitive, shielded and unshielded electronic components and subsystems, as well as registering in solid state and other detectors, and photographic films and other emulsions. Because these spacecraft responses are of particular importance for long-term interplanetary and planetary missions (especially far from the earth's orbit), thorough descriptions of charged particle intensity and fluence and their dependences on time, position and particle kind and energy are needed.

The criteria developed here complement space vehicle design criteria for the related environments of solar electromagnetic radiation and trapped radiation belts of the earth and the outer planets, published in part in NASA SP-8005, SP-8069, SP-8091, and SP-8103.

2. STATE OF THE ART

The environment of interplanetary charged particles has three components, two steady and one sporadic, namely the solar wind, solar particle events, and galactic cosmic rays. The following sections review current state-of-the-art knowledge of these components in order of increasing particle energy. Definitions of symbols and a glossary are included among the appendices.

2.1 Solar Wind

The solar wind is a fully ionized plasma which steadily streams outward from the sun in an approximately radial direction. The mass and energy flux are dominated by the proton component, for which typical densities and flow speeds are 5 cm^{-3} and 400 km/s (corresponding to a proton energy near 1 keV). Heavier nuclei, electrons, and the interplanetary magnetic field participate in the flow as well. The flow characteristics are variable, and represent a very minor contribution to the overall budget of the sun, as the mass lost annually to the solar wind is about 10^{-14} times the sun's mass and the power in solar wind kinetic energy is between 10^{-7} and 10^{-6} times that in electromagnetic radiation (sunlight).

2.1.1 Theory

Some of the important properties of the solar wind were predicted, before in-situ interplanetary observations occurred, based on theoretical considerations and indirect observations (sec. 2.1.2). The theories, introduced by Parker (1958) and refined since by many others (for a review, see Brandt, 1970), are based on the origin of the solar wind in the sun's chromosphere, where ionization and heating occur by acoustic or magnetic noise coupled to turbulence in the underlying photosphere. Because back-pressure from the interplanetary medium is negligible the hot plasma expands radially, being manifested first as the corona, and then (beyond some ten solar radii) as a supersonic (relative to the speeds of acoustic and Alfvén waves) expansion, for which the spherical divergence and the sun's gravity lead to acceleration analogous to that which governs rocket exhaust flow through a nozzle.

Theoretical solutions of the hydrodynamic equations which describe such a flow, using as input data conditions near the sun, predict average values for the density, velocity and temperature of the plasma near the earth's orbit close to observed values. Confidence is thus established in those predictions of the theory which specify the radial dependences of these quantities (sec. 2.1.5). At large distances from the sun the solar wind presumably terminates by interacting with the interstellar medium (relatively cold, unionized gas), but the location of this heliosphere boundary is not well determined either from theoretical considerations (sample recent analyses are provided by Bhatnagar and Fahr, 1972, and by Axford, 1972) or on observational ground (although a lower limit of 3.5 AU exists, sec. 2.1.2). For present purposes a conservative approach is adopted here which ignores this boundary, equivalent to the assumption that the solar wind extends to infinity.

Calculated recombination lifetimes are so much larger than flow times to several AU from the sun that the solar wind plasma remains effectively fully ionized throughout interplanetary space. This plasma behaves in many respects as a fluid and transports magnetic fields from regions near the solar surface radially away, into interplanetary space. The combination of this transport and the solar rotation leads to an interplanetary configuration of magnetic field lines, each of which resembles an Archimedes spiral, in an even number of sectors rotating with the sun, and having alternating polarity (magnetic field directed approximately inward or outward along the spiral on the average). As modified by solar wind streaming (sec. 2.1.4), this general structure is verified by spacecraft magnetometer observations (sec. 2.1.3.4).

2.1.2 Indirect Observations

Type I (ion) tails of comets interact dynamically with the solar wind, indicating its pressure and effect at distances up to a few AU from the earth and from the ecliptic plane. Quantitatively, however, the evidence for solar wind properties is partially obscured by the individual characteristics, time variability, and selection effects of the comets in the observed samples. The major pertinent conclusions from such analyses, abstracted from Brandt (1967)

and Axford (1968), are (a) the solar wind extends to all ecliptic latitudes and to at least 3.5 AU from the sun and (b) the solar wind velocity always exceeds 150 km/s, correlates with indices of geomagnetic activity (e.g., ΣK_p) and has mean radial and azimuthal components of 500 km/s and 5 to 10 km/s respectively, the latter in the direction of solar rotation.

Complementary to comet-tail observations (which yield information on the massive, proton component of the solar wind) the electron component is responsible for the scintillation (at 0.1 to 10 Hz) of small diameter radio sources. The observations (Cohen *et al.*, 1967) have been interpreted as fluctuations, on a scale near 100 km, in the electron density of $(0.14\ \mathrm{cm}^{-2})S^{-2}$, for the region $0.2 < S < 0.9$ AU from the sun; these conclusions are supported, with a modestly different dependence on S, by the scintillation discussion of Hewish and Symonds (1969).

Additional indirect information on solar wind properties can be inferred (Axford, 1968) from the time delay between disturbances on the solar surface (e.g., flares) and geomagnetic disturbances (e.g., sudden commencements), yielding wind speeds; from various aspects of geomagnetic disturbances yielding solar wind variability information; from the polarization of zodiacal light, yielding electron density; from the green coronal emission lines, yielding plasma emissivity and temperature near the sun; from solar Lyman-α radiation scattered by neutral hydrogen, yielding some interaction characteristics between the plasma densities and the neutral gas; from dynamic spectra of solar radio bursts, yielding plasma densities and temperatures near the sun; from scattering of extended radio source emission, yielding electron densities and plasma filamentary structure; from radar (ground based) and satellite radio transmissions, yielding electron density and its fluctuations; and from cosmic ray variations, yielding information on solar wind-carried magnetic field fluctuations. Most of the inferences are not discussed further here, as they are consistent with the results of spacecraft observations, which provide more detail and reliability for the quantities involved.

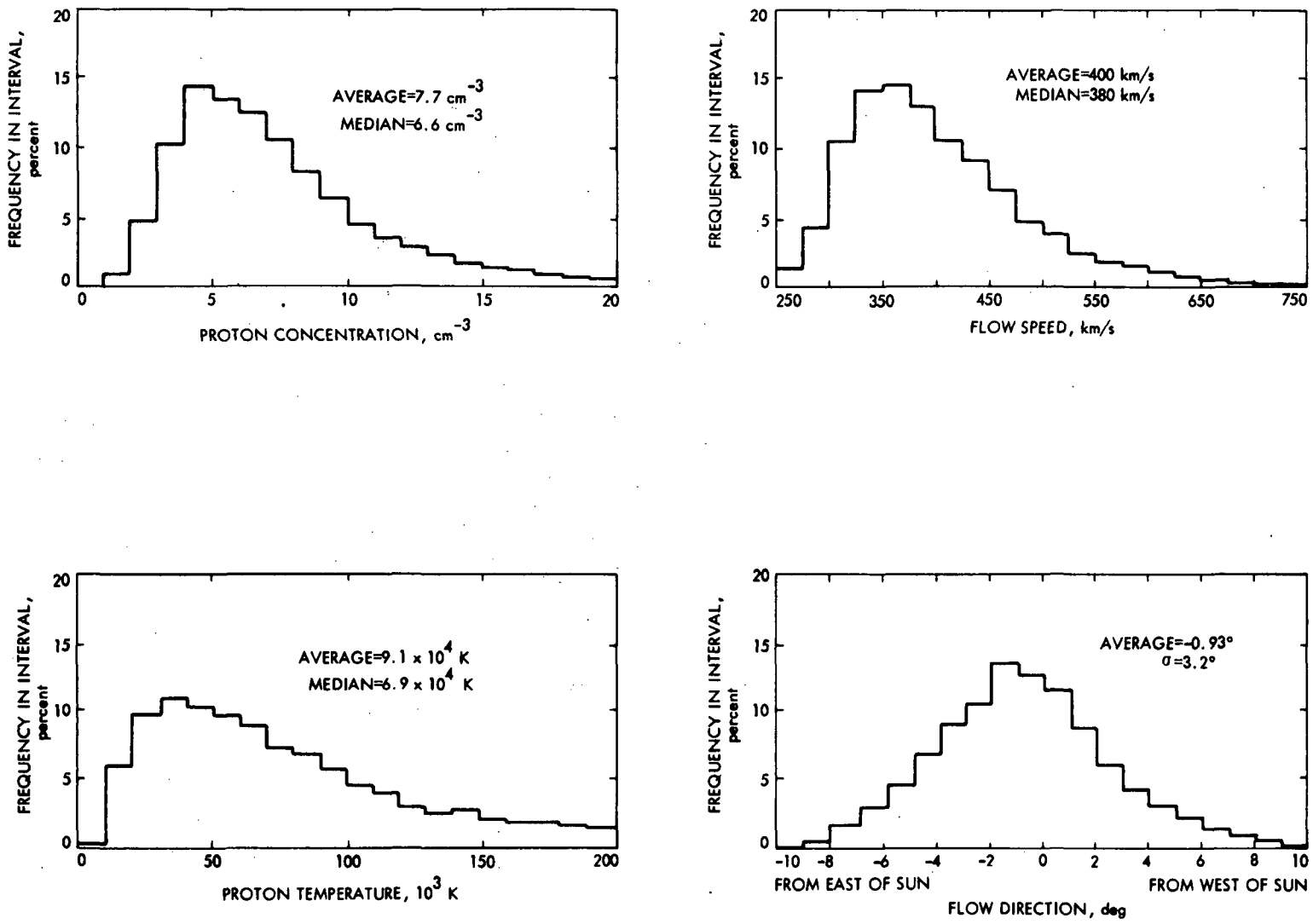

Figure 1. Sample distributions of proton characteristics in the solar wind near 1 AU. Data measured in 1965-1967 by the electrostatic analyzer systems on the Vela 3 (A and B) satellites (Hundhausen *et al.*, and Wolfe, 1972).

2.1.3 Direct Observations

Numerous spacecraft-borne instruments, including particularly plasma cups, electrostatic analyzers, charged particle telescopes, and search coil and flux gate magnetometers, perform in-situ measurements of solar wind properties in interplanetary space (beyond the earth's magnetosphere). These include earth-orbiting satellites with apogee distances greater than about 60,000 km (ten earth radii), notably members of the IMP (Explorer) and Vela series, HEOS I, and OGO V; lunar orbiters and landers, notably Explorer 35; and planetary and interplanetary vehicles, notably members of the Pioneer and Mariner series.

Various aspects of the solar wind derived from data taken near the earth's orbit are discussed in the following sections.

2.1.3.1 Proton Properties

Figure 1 (adapted from references cited in the caption) includes sample histograms of proton concentrations, flow speed, flow direction, and temperature. In each case the most probable, median and mean values increase in that order. To within about a factor 2 (typical of the upper limit for differences among various experiments), representative proton values are 5 cm^{-3} for the concentrations, 400 km/s for the flow speed, 1 degree prograde for the angular departure from the radial, and 10^5K for the temperature. Additional real details in the distributions of considerable scientific interest, particularly the slight proton temperature anisotropy, are ignored here because they are masked, for the purposes of spacecraft environmental design criteria, by the large variability in these quantities.

2.1.3.2 Heavier Ions

Figure 2 is representative of composition measurements, as reviewed by Bame (1972), and shows that ions heavier than He^{++}, while present in the solar wind, are negligible in comparison to protons in terms of concentration and mass and energy flux. They will thus be ignored here. Histograms for the concentration, flow speed and direction, and temperature of the He^{++} ions

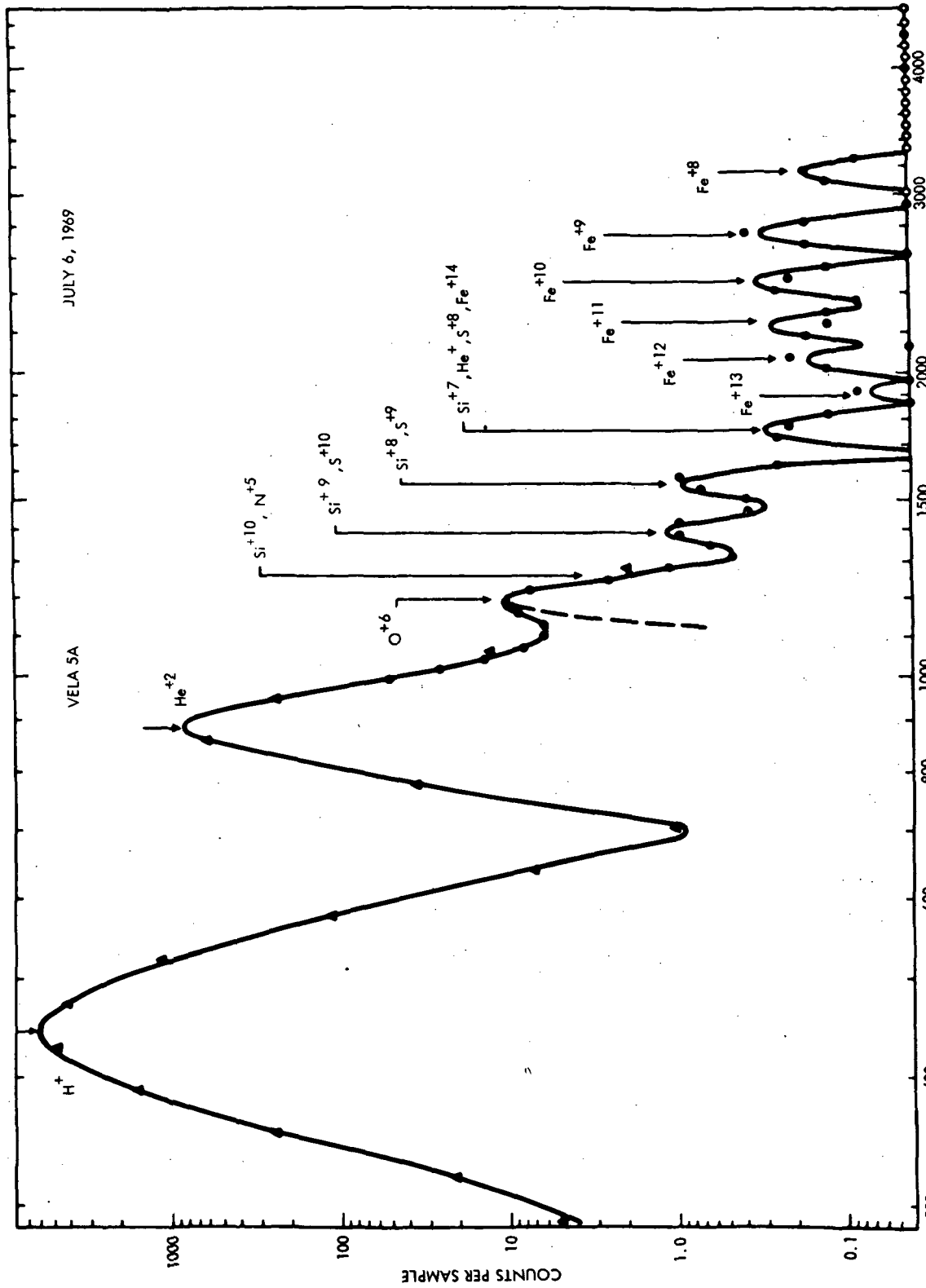

Figure 2. Sample distribution of ion species in the solar wind near 1 AU. Data measured 6 July 1969 by the solar wind (triangles) and heavy ion (dots) analyzers on Vela 5A (Bame *et al.*, 1970, and Bame, 1972).

strongly resemble those for the protons if the proton concentrations are multiplied by about 0.05 and the proton temperatures are multiplied by 4. Thus both the flow and thermal velocities are approximately independent of ionic specie in the solar wind.

2.1.3.3 Electrons

Montgomery (1972) reviews the available electron data, which imply that the electrons participate in the bulk flow with velocity identical to, and having the concentration required for charge neutrality with, those of the ionic species locally. The corresponding electron concentration and flow histograms are thus comparable to those shown in fig. 1 for the protons, with variations in phase with the protons. The electron temperature, however, is less variable than the proton temperature, and is almost always between 10^5 and 2×10^5 K, with negligible anisotropy; thus the electron kinetic energy ($\sim$ 20 eV) is primarily thermal rather than associated with the plasma flow.

2.1.3.4 Magnetic Fields

Figure 3 includes histograms of magnetic field strength and orientation, from the discussion by Ness *et al.* (1971). Typically, the field is about 5 nT (5 gamma, or 5×10^{-5} Gauss) directed inward or outward along a line about 45° west of the sun. The field reverses direction rather abruptly at irregular intervals (typically one week) and is consistent with the spiral and sector structure expected theoretically (sec. 2.1.1).

2.1.4 Dynamics

Significant correlations among proton concentration, flow speed, and temperature are shown in fig. 4 (adapted from data reported by Hundhausen *et al.*, 1970). Similar correlations are discernible in measurements on almost any time scale from seconds to days and are commonly discussed in terms of plasma streams which originate near the sun (having, of course, some basis in solar activity), and move radially away. Among such streams high concentrations generally accompany low flow speeds and proton temperatures, such that mass and

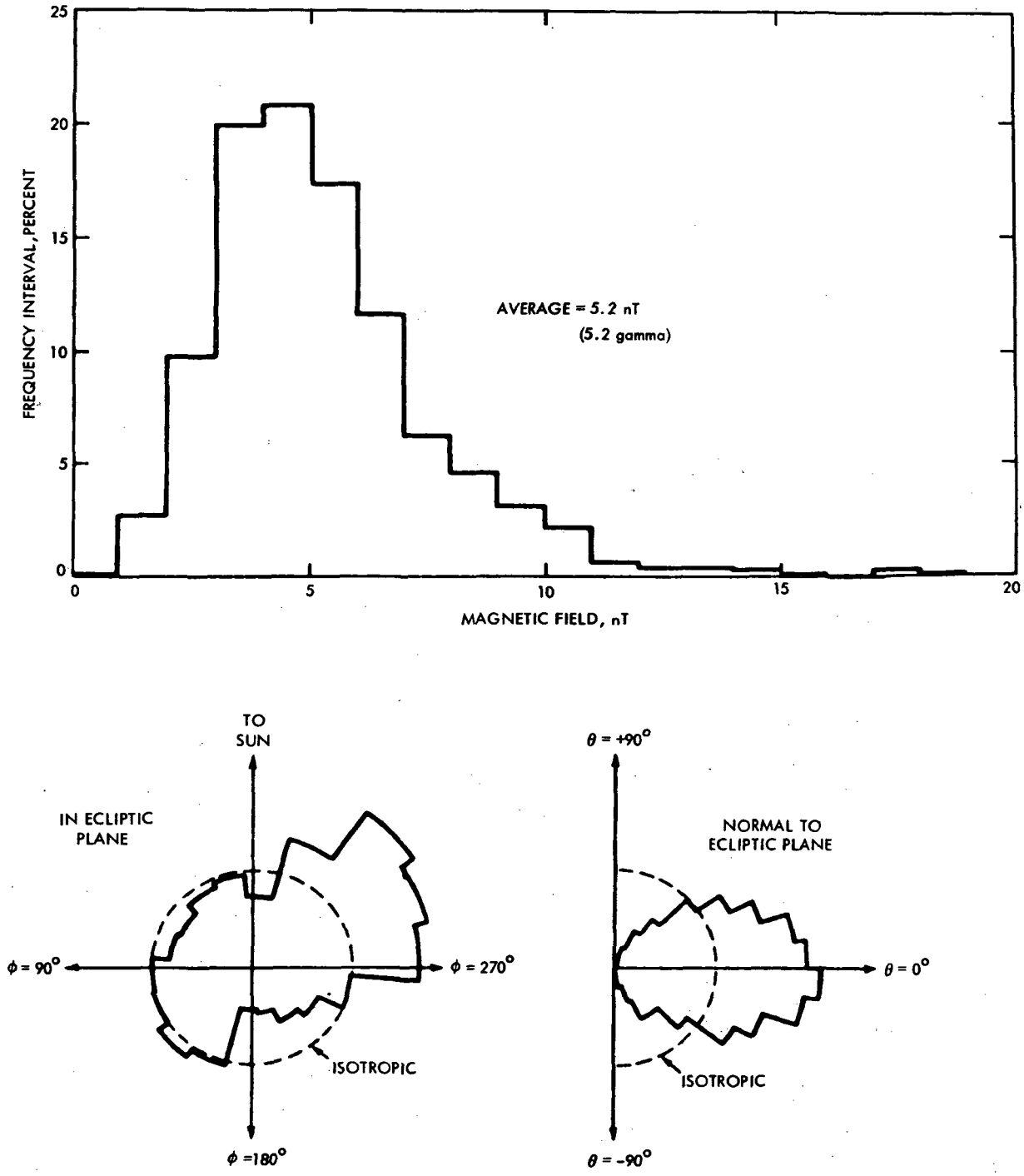

Figure 3. Sample distribution of magnetic field strength and direction in the solar wind near 1 AU. Data measured in 1965-1967 by the magnetometer on IMP 3 (Ness *et al.*, 1971).

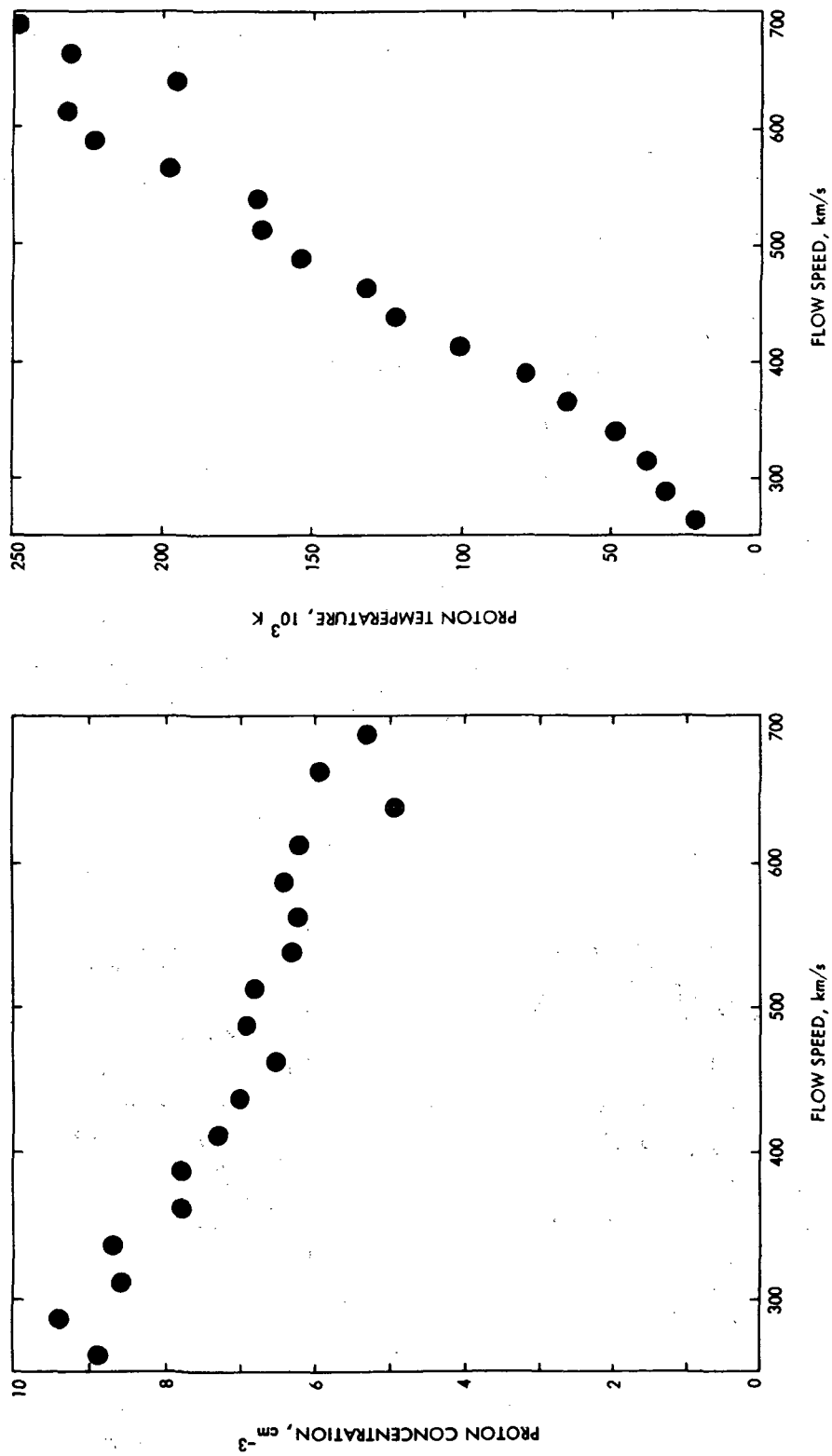

Figure 4. Sample correlations among proton characteristics in the solar wind near 1 AU. Data sources identical to those for fig. 1.

energy fluxes in the solar wind are more nearly uniform than either the concentration or flow speed. The concepts of such streams and interactions among them (particularly when a fast stream overtakes a slow one) modify the simple theoretical picture (sec. 2.1.1) of the solar wind and magnetic field, and lead to some understanding of the large variations seen in the plasma and field configuration data (Davis, 1972, and others).

A complementary view of the dynamics of the solar wind is provided by a look at the various time scales for variations in solar wind properties. Variations which occur on time scales less than or of the order of an hour (the microstructure), serve as data bases for the understanding of detailed interactions (including waves) in the solar wind and represent convection past the observer of regions with different plasma properties (Burlaga, 1972). Variations on time scales of the order of a week (large scale and sector structure, sec. 2.1.1) represent the rotation past the observer of stream source regions on the solar surface (period about 27 days; Wolfe, 1972). Variations on time scales of a few years could be associated with the 11-year cycle of solar activity, although predictions of specific variations in solar wind properties are not practicable on a long-term basis. Thus the short-term variations cover the full range of plasma properties, and those ranges and the corresponding distributions do not display marked long-term changes on the basis of available data.

2.1.5 Radial Dependences

Spacecraft observations carried out between the orbits of Venus and Mars display no significant variation of the plasma velocity and temperature distributions with heliocentric distance S, but the concentration distributions are consistent with an S^{-2} dependence (Neugebauer and Synder, 1966). These results are limited by the large variability in solar wind properties at one value of S (namely the earth's orbit) and by the relatively small range of S available to the experiments. They are generally consistent with a variety of theoretical analyses, among which Cuperman *et al.* (1972) is exemplary because

of its emphasis on radial dependences and its citation of most other prominent analyses. In interplanetary space (i.e., more than several radii from the sun) simple power law dependences are adequate for present purposes, so we adopt proportionalities of S^0 (independent of S) for plasma velocities, S^{-1} for temperatures and magnetic field strengths, and S^{-2} for concentrations.

2.2 Solar Particle Events

Occasionally protons with energies of the order of 10 to 100 MeV propagate in interplanetary space following acceleration near the sun. Because solar particle events generally occur subsequent to flares on the sun's surface, flare eruption and proton acceleration and/or release probably share an origin in local instabilities of the plasma and magnetic field configurations within active regions on the sun, usually associated with sunspots. Such protons are variously referred to as solar flare protons or solar cosmic rays. Discussion of associated electrons is deferred to sec. 2.2.6.

2.2.1 Observations

The presence of energetic solar particles near the earth has been inferred from various ground-based instruments, notably neutron monitors, ionization chambers, and riometers, and from charged particle detectors carried in balloons, aircraft, and earth satellites. The data so acquired, however, include modifications which result from particle interactions with the earth's magnetosphere and atmosphere. More direct data are fortunately available from charged particle detectors on earth orbiting satellites with apogees outside the magnetosphere and on interplanetary spacecraft, notably IMP and Pioneer. Although some protons in the energy range of interest are commonly present (of both galactic and solar origin), flux enhancements of several orders of magnitude occur in relatively distinct events at very irregular intervals. In many months, for example, no events are detected, but in others one to six occur, such that an average rate of occurrence is of the order of one event per month.

During such an event, particle intensities at and above some particular energy follow a rapid rise (commonly a few hours) and a slower decrease and disappearance (commonly several days). The time profiles and the development of the spectra are characteristic both of the individual event and of the detector trajectory, displaying great variety (McDonald, 1963). The integration of the intensity over solid angle and over the duration of the event leads to values for the fluence at various proton energies. Recurrences of proton detection about 27 days (one solar rotation) following the original event have also been observed, but the recurrent intensities are orders of magnitude smaller than the original ones.

The angular distributions derived from charged particle telescope data are strongly variable as well, as summarized, for example, by McCracken *et al.* (1968). The anisotropy commonly ranges between 0.2 and 0.5 early in an event, with the variable direction of maximum intensity often parallel to the interplanetary magnetic field. Later in the event (say after the peak intensity) the anisotropy is commonly smaller, e.g., 0.1, indicating a more nearly isotropic intensity. Because the dependence of the intensity on direction is so variable and because the intensities are so variable in time and the events are so sporadic, it is not worthwhile to include directional effects directly in an engineering model, their variations being masked by other uncertainties.

2.2.2 Theory

Several authors have discussed mechanisms for processes near the sun which result in particle acceleration, storage, injection, and/or leakage. The application of the results of such theories for the origin of solar particles is limited by the major modifications in particle populations which result from various mechanisms of particle transport in interplanetary space. These mechanisms include convection, adiabatic deceleration, anisotropic diffusion, interaction with a diffusion region external boundary, and possibly others. Their theoretical treatment is commonly handled using a Fokker-Planck equation, and the complexity of the relationships among position, time, energy, intensity, fluence, and various input parameters (e.g., in the diffusion coefficients and boundary conditions) suggests that numerical solutions are appropriate. Aspects of such theories, their development in the literature, their numerical solutions, and comparisons with the observations have been published by Englade (1971) and Webb and Quenby (1973), among others.

Both the complexity of the theory and the individuality of particular events suggest that the successes of the theoretical and numerical treatments are not suitable for the overall engineering descriptions needed here. For this purpose we concentrate on the peak intensity and fluence for an event as functions of energy and heliocentric distance, ignoring the time profile, and angular and heliocentric longitude dependences. Average energy spectra, at

least near the earth's orbit, can be obtained from spacecraft data which cover numerous events, but only a few events have been observed at widely separated positions so that inferences about position dependences are confused by the individuality of the events observed. Further, the position dependences may be different at different energies, as the relevant transport mechanisms assume different relative importances.

To provide a suitably simple model, three ad hoc assumptions, only loosely tied to the results of the theoretical treatments, are adopted here. First, particle acceleration and loss in interplanetary space are ignored, so that energy spectra are independent of position. Second, any angular spreading of the particles (as they move a distance S from the sun) is ignored, so that, to avoid long-term changes in the particle content of interplanetary space, a fluence proportional to S^{-2} applies to events on the average. Third, to simulate the fact that diffusion in the general direction of the particle trajectory is more rapid than perpendicular diffusion, the radial extent of a group of particles is taken as proportional to S, such that the peak intensity is proportional to S^{-3} (inversely proportional to the volume occupied by the particles) for events on the average. Some alternative, energy-dependent relations, and further references are discussed by Thomas (1972) and by Haffner (1972).

2.2.3 Correlations and Predictions

The association of solar particle events with solar flares and other manifestations of solar activity has prompted searches for correlations of event severity and/or rate (or probability) of occurrence with other indices of solar activity, notably sunspot number. For this purpose tables are needed which summarize data from many events on a common basis, and the most useful summaries are those which provide the peak intensity and the fluence of protons above various energy values for each event exceeding some threshold. For cycle 20, between 1964 and the present, such a tabulation is provided by Atwell (1972) from spacecraft experiments (IMP and Explorer) exclusively. For cycle 19, between 1954 and 1964, such a tabulation is provided by Weddell and Haffner

(1966), which extends the ground-based, balloon and satellite data compiled by Webber (1963) through 1963. Prior to cycle 19, insufficient data on solar protons are available for useful analysis.

Some of the above data compilations (and others) include various other facets of solar activity, e.g., observed details of associated sunspots, flares, plages, and radio frequency bursts. Correlations of such data with solar particle event observations permit short-term predictions of solar particles on time scales from weeks to hours in advance, with modest accuracy. Such predictions are useful in spacecraft operations (Gonzalez and Divita, 1968) but for spacecraft (and mission) design purposes long-term predictions are needed. The available techniques quantify the correlations of event probability of occurrence and severity with solar activity and use the results for prediction purposes, leading examples being Burrell (1972), Dollman and Bechtelheimer (1967), Roberts (1966), Thomas (1972), Wilson (1971), and Yucker (1972). These predictions serve specific purposes, particularly including calculations of radiation dose for manned missions, but are based entirely on data from solar particle events in cycle 19 and are restricted to the vicinity of the earth's orbit (except for Thomas, 1972, and Yucker, 1972). Certain features from these last two articles have been included in the following development of a new and complete probabilistic description, notably a correlation of particle activity with sunspot number. The new prediction technique also includes the following features: solar particle event data from both cycles 19 and 20; continuous (rather than discrete) values for energy, intensity, fluence, and probability; and a formulation which permits applicability to interplanetary missions with arbitrary time profiles of heliocentric distance.

2.2.4 Reduction of Proton Data

The data tabulations discussed above provide peak intensities and fluences above three energies for 67 events between 1 June 1956 and 30 September 1964 (during cycle 19) and 38 events between 1 April 1967 and 31 March 1970 (during cycle 20). To construct the new model for probabilities of event occurrence, peak intensity, and fluence, these data were divided into six time intervals, each containing about 18 events, and for each interval a fluence plot and a peak intensity plot similar to fig. 5 were made. The average sunspot number R_z was calculated for each such interval from data published regularly in *Solar Geophysical Data*, Part I, and intervals with similar average sunspot numbers were combined, yielding three plots, of which fig. 5 is a sample; this was possible because among the original plots those with comparable sunspot numbers were very similar, even those from different solar cycles. It was possible to approximate most of the 315 entries for the numbers $N(I)$ of events versus peak intensity I (with energy > E) to within $[N(I)]^{\frac{1}{2}}$ by the numerical formula

$$N(I) = \sum C \exp[-3.69(S^3 I E^{1.55}/1.56\times10^9)^{\gamma_1}] \quad (1)$$

Here the symbols and units are specified in Appendix A, the summation extends over the months in the interval, and C and γ_1 are given by

$$C = \text{smaller of } [1.0, (1/6)\exp(R_z/42)] \text{ per month} \quad (2)$$

and by

$$\gamma_1 = \text{larger of } [(468-R_z)/1450, (R_z-36)/275]. \quad (3)$$

Similarly, it was possible to approximate 210 of the 315 entries for the number $N(F)$ of events versus fluence F to within $[N(F)]^{\frac{1}{2}}$ by the numerical formula

$$N(F) = \sum C \exp[-3.85(S^2 F E^{1.87}/6.94\times10^{15})^{\gamma_2}] . \quad (4)$$

Here C is given by eq. 2 and γ_2 by

$$\gamma_2 = \text{larger of } [(289-R_z)/819, (R_z-50)/243]. \quad (5)$$

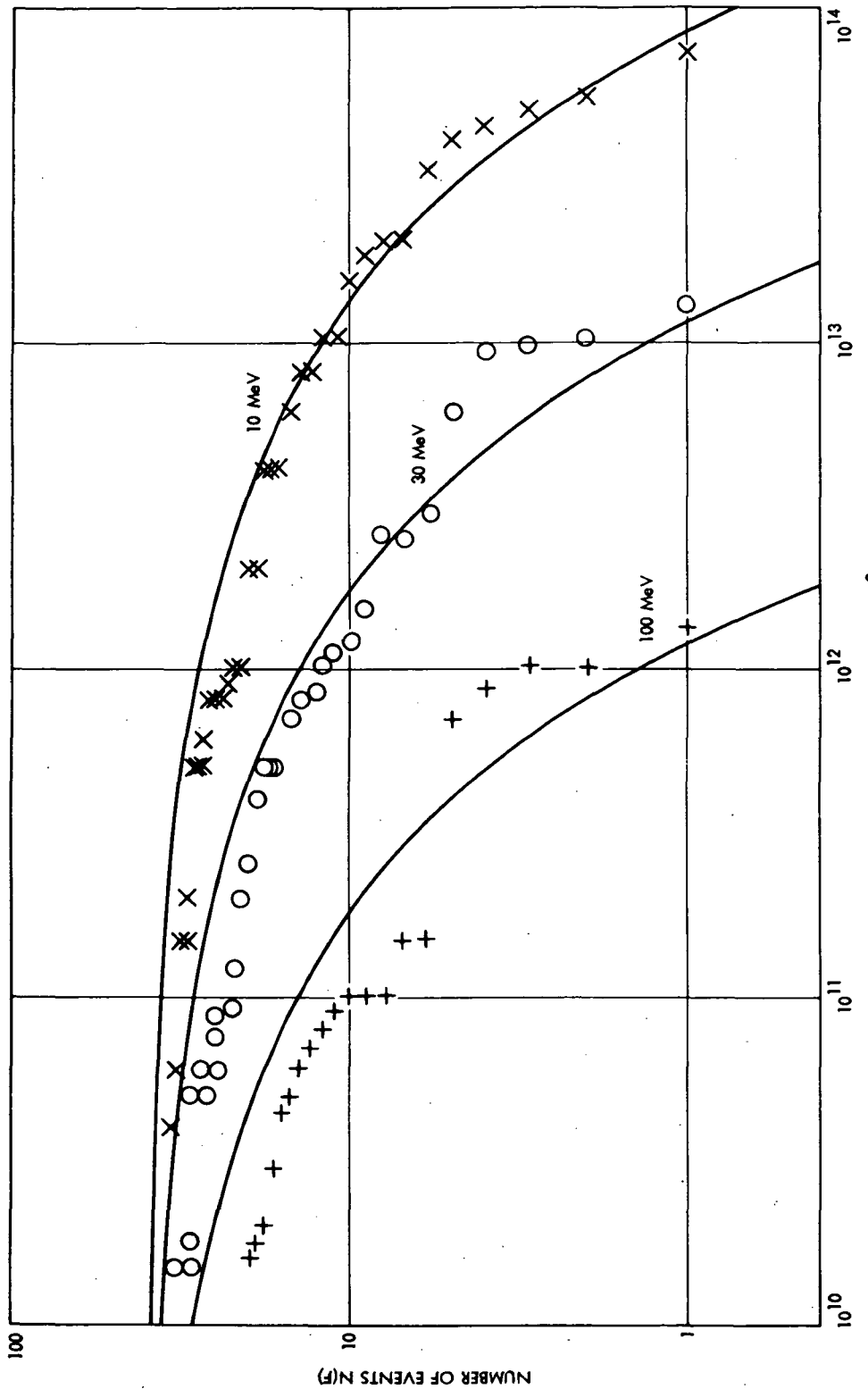

Figure 5. Data and predictions for solar particle events with fluence exceeding F, for protons above three energies, for the interval June 1956 through October 1959.

Expected numbers of events at several energies and fluences, calculated using eq. 4, for the sample interval at the earth, are included in fig. 5 for comparison with the original data.

2.2.5 Long-Term Probabilities

The sporadic occurrence of solar particle events suggests that the Poisson distribution may be used for long-term prediction, even though, strictly, a uniform probability of occurrence does not pertain. This approach leads to an expression for the probability that the peak intensity I will be exceeded in the form

$$P(I) = 1 - exp\ [\ -N(I)]. \tag{6}$$

Here we have assumed that eq. 1 for $N(I)$ can be used to predict the mean number of events in a time interval, and that the observed event rates in the base time intervals are mean ones for the particular conditions, as described by the sunspot number.

The expression (comparable to eq. 6) for the fluence probability is much more complex, because every event contributes to the fluence (for the peak intensity, only the severest event at the energy of interest contributes). Appendix C outlines the derivation of the probability that the fluence F will be exceeded in the form

$$P(F) = \sum_{\ell=1}^{\infty} \left\{ 1 - [e^{-N_o}] \sum_{k=0}^{\ell-1} N_o{}^k/k! \right\} D_\ell(F) \tag{7}$$

Here

$$N_o = N(F) \text{ at } F = 0, \tag{8}$$

$$D_1(F) = N(F)/N_o \tag{9}$$

and

$$D_\ell(F) = N_o{}^{-1} \int_0^F [-dN(x)/dx] D_{\ell-1}(F-x)\ dx. \tag{10}$$

This last expression must be evaluated for a sufficient number of terms; usually terms for which $\ell \geq (N_o + 20)$ contribute less than 10^{-4} to $P(F)$. Equations 7 through 10 are comparable to expressions derived by Yucker (1972), where sums are presented for $[1-P(F)]$.

The expressions presented above permit calculations to be performed for any mission and/or time interval, if the actual smoothed or predicted sunspot number R_z is available. Values for R_z specified in *Solar Geophysical Data*, Part I, are appropriate here, and mean cycle values may be used beyond the limit of the tabulation provided there. The formulation is continuous in E, I, F and probability, and yields reasonable results in the ranges $30 \leq R_z \leq 180$, $10 \leq E \leq 100$ MeV, $10^3 \leq I \leq 4\times10^7 m^{-2}s^{-1}sr^{-1}$ and $10^{10} \leq F \leq 10^{14} m^{-2}$; these are the ranges of the data used in the fitting procedures. For values beyond these ranges the formulation is probably reasonable as long extrapolations to extremes such as $R_z \geq 250$, $I \geq 10^9 m^{-2}s^{-1}sr^{-1}$, or $F \geq 10^{15} m^{-2}$ are avoided.

Sample results, generated by a computer program which evaluates the quantities appearing in eq. 6 through 10, are shown in fig. 6 for the Mariner-Jupiter-Saturn 77 mission (JST trajectory). Fluence probabilities from eq. 7 are shown for three energy values. Comparable calculations can be completed for peak intensities and mission fluences for any interplanetary mission.

2.2.6 Other Particles and Energies

Components of solar particle radiation other than the solar wind and solar flare protons in the energy range of a few to a few hundred MeV are less fully treated in the research literature. Their development here is accordingly brief.

For energies above 100 MeV, an extrapolation of the description of sec. 2.2.4 and 2.2.5 for solar protons is appropriate until they are dominated by primary galactic cosmic rays (at $E \sim 1000$ MeV, sec 2.3). In the energy interval between the solar wind and solar proton events (e.g., $10^{-3} < E < 10$ MeV) a peak integral intensity of $I = (10^8 m^{-2}s^{-1}sr^{-1})/S^3E^{1.2}$ approximately matches

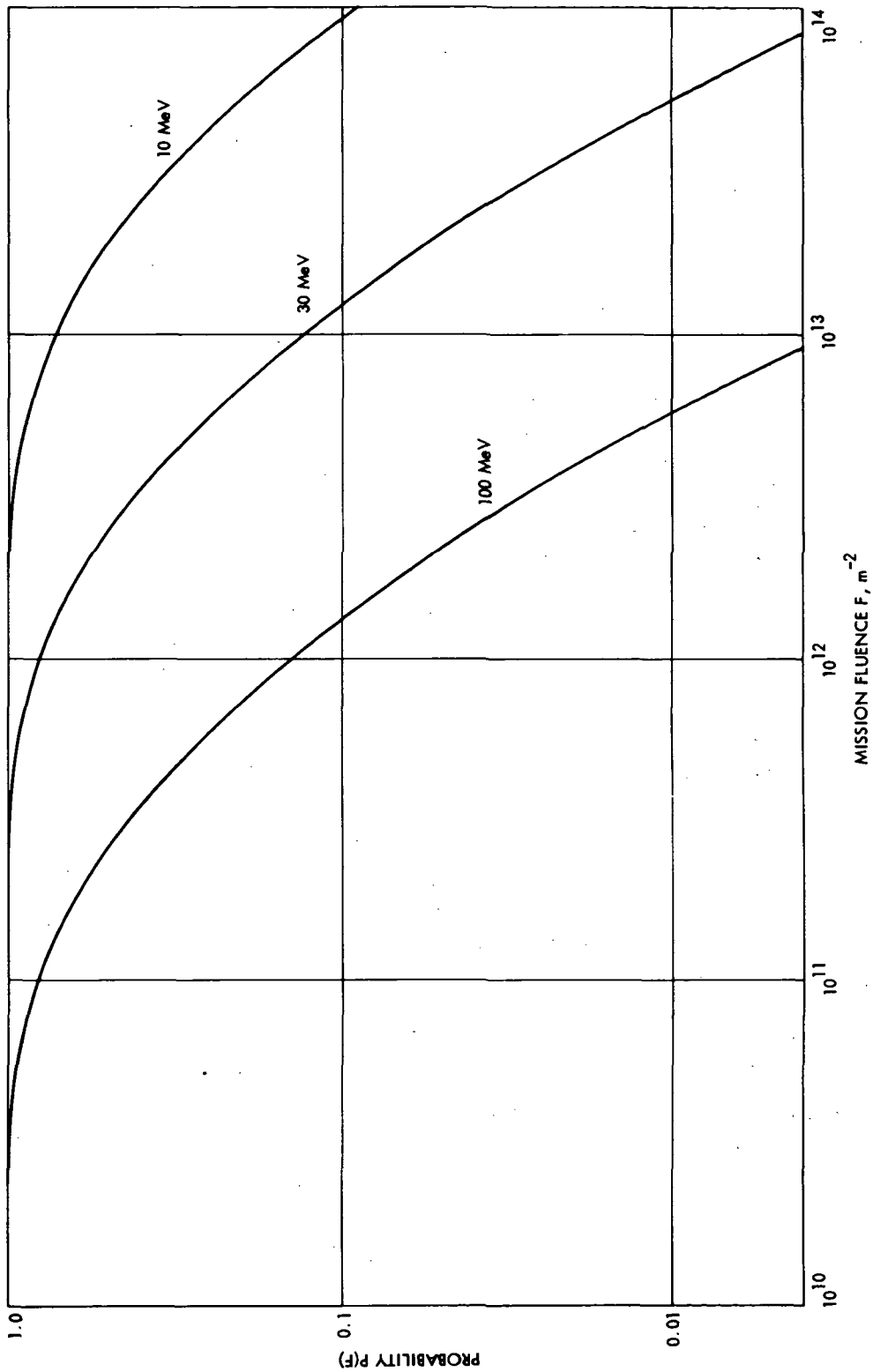

Figure 6. Prediction of probabilities for mission fluence exceeding F, for solar protons above three energies, for the MJS'77 mission (JST trajectory).

both a high solar wind value and a typical solar proton event. In the same interval an average integral intensity of $I = (10^6 m^{-2} s^{-1} sr^{-1})/S^2 E^{1.7}$ approximately matches both a typical solar wind value and average fluence accumulation rate from solar proton events. In these crude approximations the heliocentric distance S is in AU and the proton kinetic energy E is in MeV for the range $10^{-3} < E < 10$ MeV.

Nuclei other than protons are present in solar particle events, but intensity ratios are less than or equal to that of helium, for which an intensity 0.05 times that the protons is reasonable for both the solar wind (sec. 2.1.3.2) and solar particle events (Dietrich, 1973).

Cline and McDonald (1968) describe the 3 to 12 MeV electron component of several solar particle events as observed by IMP 1 and 3. Typical peak intensities are 1 $cm^{-2} s^{-1} sr^{-1}$ in this energy range, for which they (McDonald *et al.*, 1972) feel a differential spectrum proportional to E^{-3} is appropriate. A peak integral intensity approximation $I = (10^5 m^{-2} s^{-1} sr^{-1})/S^3 E^2$ matches these properties and when extrapolated to lower energies is comparable to the largest observed intensity tabulated by Lin and Anderson (1967) for electrons with energy $E > 40$ keV. If a duration of 10^4 s and a rate of the order of once per month are adopted for such a solar event electron intensity, an average integral intensity approximation $I = (400\ m^{-2} s^{-1} sr^{-1})/S^2 E^2$ is comparable both to the galactic cosmic ray electron intensity above 1 MeV (some of these may be solar; a discussion is given by McDonald *et al.*, 1972) and to the intensity of electrons in the solar wind (thermal energy about 20 eV; sec. 2.1.3.3). In these crude approximations the heliocentric distance S is in AU and the electron kinetic energy E is in MeV for $2 \times 10^{-5} < E < 10$ MeV. At higher energies galactic cosmic ray electrons (sec. 2.3) dominate.

2.3 Galactic Cosmic Rays

Galactic cosmic rays are relativistic charged particles (electrons and atomic nuclei) which continuously penetrate the solar system from external sources (as contrasted with those of solar origin or in planetary radiation belts). Individual particle energies range from about 1 to 10^{14} MeV, and typical energy densities for the entire population are in the range 10^{-13} J/m^3, comparable to the energy density of electromagnetic radiation from sources other than the sun.

2.3.1 Observations

At the highest energies observed (say $\gtrsim 10^{10}$ MeV) the intensity of cosmic rays is so small ($\lesssim 10^{-8}$m^{-2}s^{-1}sr^{-1}) that it is impossible to record enough primaries for statistical significance using direct detectors of reasonable exposure. Such particles do, however, reach the earth's atmosphere with negligible interplanetary or terrestrial magnetic field deflection, and react with nuclei of air molecules, producing numerous secondaries in an extensive air shower (EAS) which can be analyzed with an array of ground-based scintillation detectors. This technique, reviewed by Sreenkantan (1972), effectively employs a large area of the atmosphere to provide sufficient exposure but does not permit the unambiguous identification of the cosmic ray primary particle kind.

At intermediate energies (10^4 to 10^9 MeV) data from ground-based instruments is supplemented by balloon-borne, and to some extent by spacecraft, experiments. Here any material may be examined for the effects of cosmic ray impact (ionization or nuclear reactions), but calibrated detectors including emulsion stacks, spectrometers, calorimeters, Cerenkov counters, and scintillators provide the most detailed data. Here the ratios of protons and helium nuclei are very similar to their values at lower energies, and the proportions of heavier nuclei, while possibly enhanced at higher energies, are still very small. The integral intensity determined from data at intermediate and high energies is reproduced in fig. 7 (Sreenkantan, 1972).

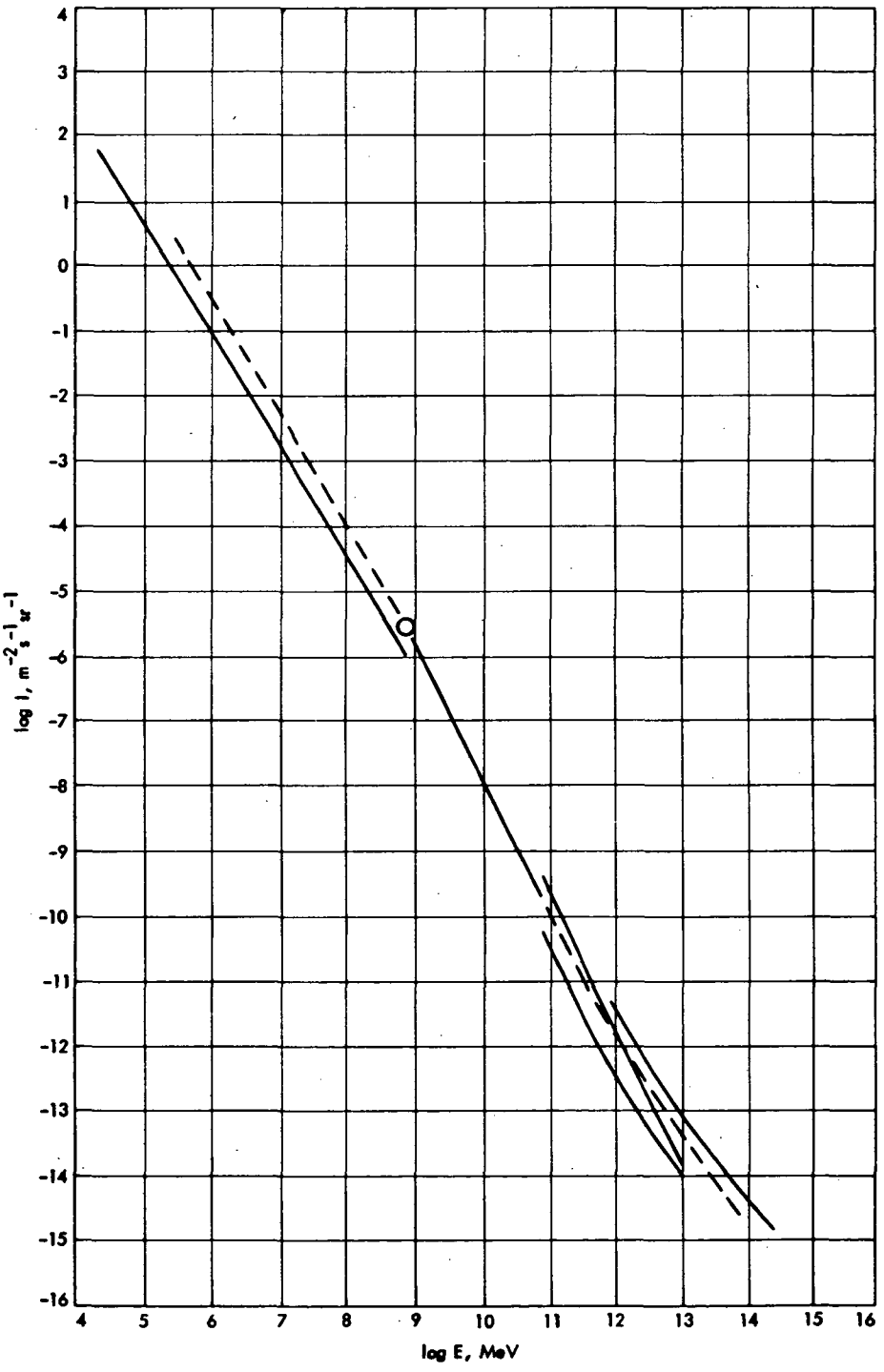

Figure 7. Composite integral intensity spectra of primary galactic cosmic rays. The entries and their sources are reviewed by Sreenkantan (1972).

At low energies ($\lesssim 10^4$ MeV) the particle intensities are affected by interplanetary and terrestrial magnetic fields, and thus display marked dependences on time and on the location of measurement. Detectors near the earth's surface, particularly neutron monitors, thus measure fluxes of secondaries (produced in the atmosphere) which vary strongly with latitude (and, to a lesser extent, with time of day). These monitors sometimes also show counting rate enhancements (during solar particle events), Forbush decreases (when solar wind streams near the earth deflect low-energy particles), and modulation within the solar cycle. Numerous other detection systems for the low energy particles and their secondaries have been deployed near the ground and within earth's atmosphere and magnetosphere.

More reliable data on interplanetary intensities of low energy galactic cosmic rays have been derived from experiments on spacecraft beyond the influence of the earth's atmosphere and magnetic field. These data come from arrays of shielded GM counters, ionization chambers, solid state detectors, scintillators, and Cerenkov detectors with appropriate pulse-height coincidence, anti-coincidence and geometric analysis (such an experiment package is known as a cosmic ray telescope) on spacecraft including IMP (Explorer), OGO, Mariners, Pioneers, and various Soviet probes. The intensities, after corrections for such problems as background, noise, solar particles, etc., are isotropic and in broad agreement among the numerous experiments; appropriate sample values for three different years are shown in fig. 8 (Hsieh *et al.*, 1971).

These several experiments are sometimes configured in ways which permit discrimination among electrons, positrons, protons, and several heavier nuclei. Among primary cosmic ray particles, protons predominate, whether comparisons are made on the basis of rigidity, kinetic energy per incident particle, or kinetic energy per nucleon. Quantitative comparisons are commonly made on this last basis, and a useful, brief review occurs in Simpson (1971), from which fig. 9 is taken for helium and other nuclei. Figure 10, from McDonald *et al.* (1972), provides comparative differential intensity spectra for electrons, positrons, protons, and helium nuclei.

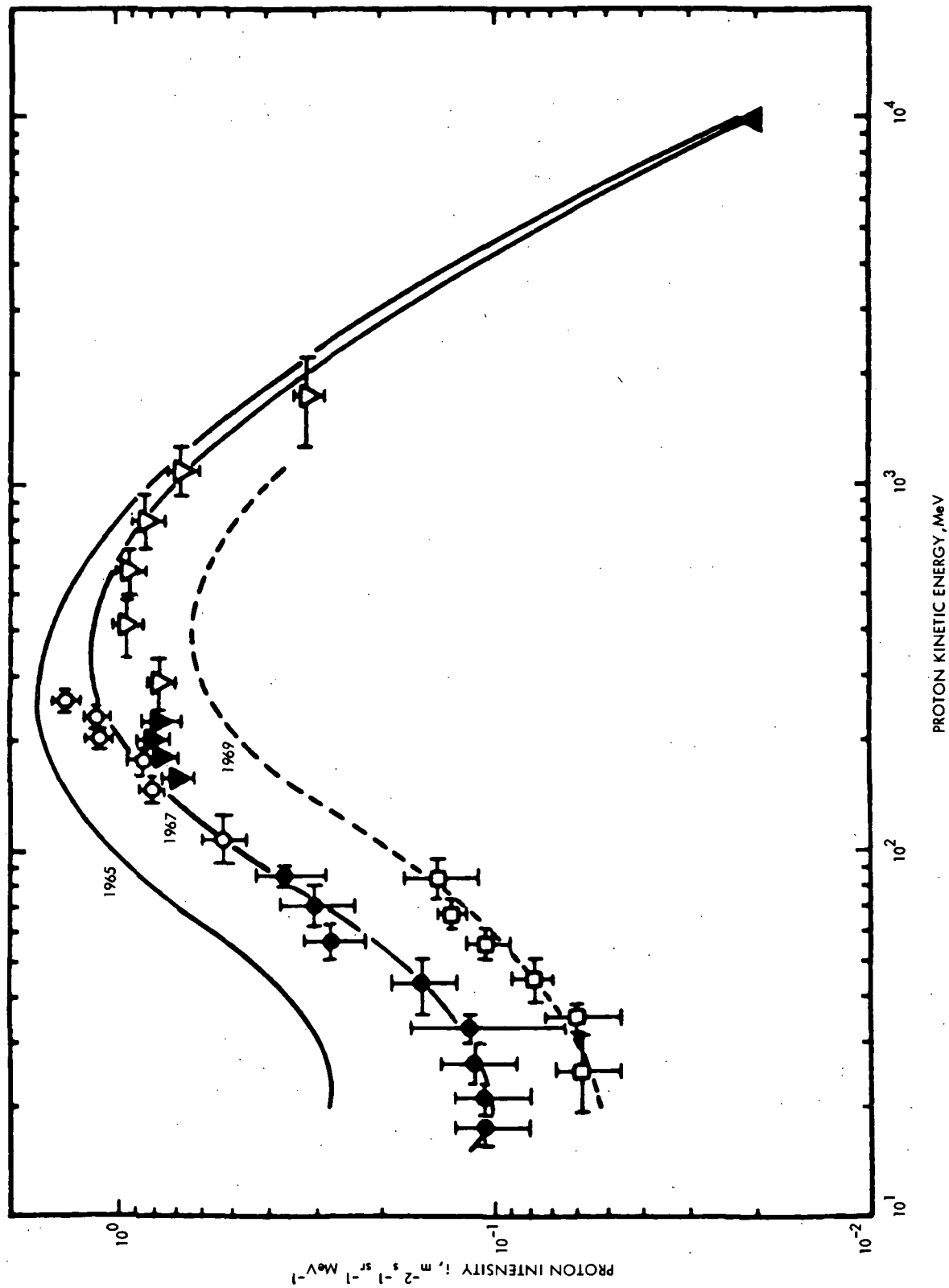

Figure 8. Composite differential intensity spectra of galactic cosmic ray protons. The entries and their sources are reviewed by Hsieh *et al.*, (1971).

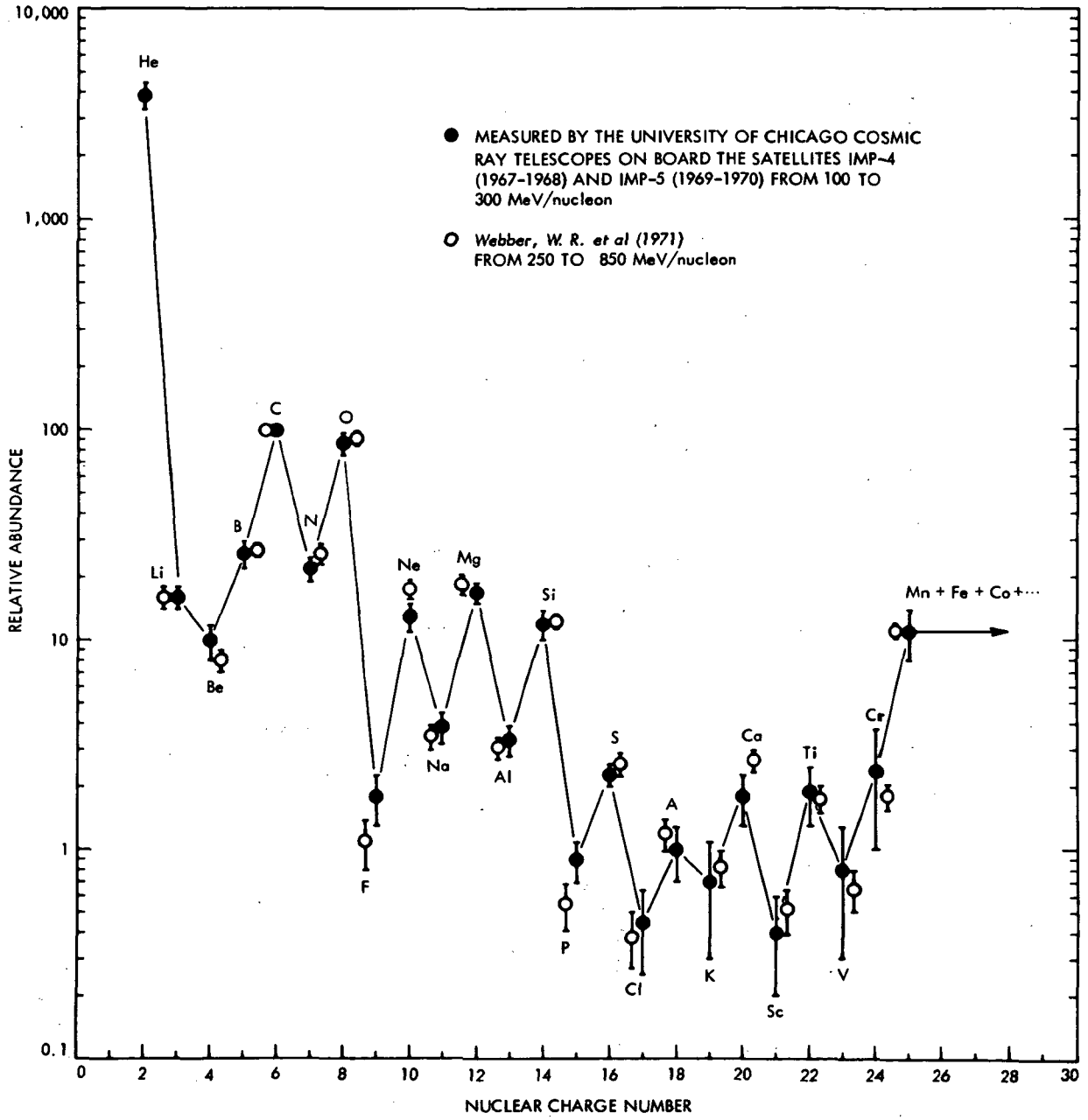

Figure 9. Relative abundances (Carbon = 100) of cosmic ray nuclei at energies below 1000 MeV/nucleon as measured by IMP 4 and 5 (Simpson, 1971).

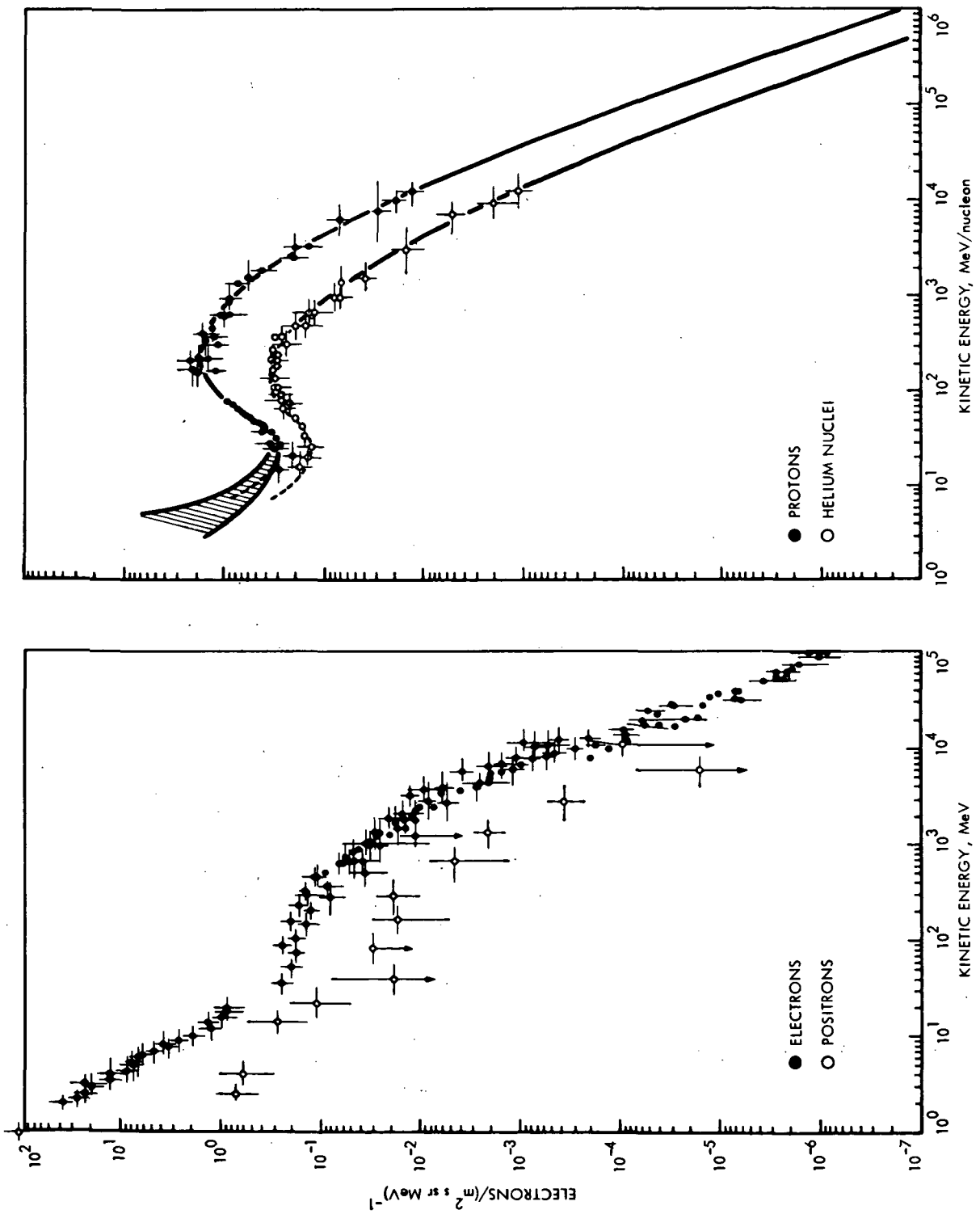

Figure 10. Composite differential intensity spectra of galactic cosmic ray electrons, positrons, protons and helium nuclei. The entries and their sources are reviewed by McDonald *et al.*, (1972).

2.3.2 Theory

Theoretical discussions of galactic cosmic rays commonly address several of the characteristics evidenced by the observations, particularly the composition, energy spectrum, and modulation. These analyses treat particle origin and acceleration (e.g., Simpson, 1971); transport and containment in the galaxy and interaction with interstellar matter (e.g., Fichtel and Reames, 1968); and convection, diffusion, and other propagation effects in interplanetary space (e.g., Jokipii, 1971). For all of these topics, however, there are major unresolved problems, and the theories do not greatly assist in the development of an engineering-oriented environmental description based rather simply on the observations. In particular, heliocentric distance variations which might support the interplanetary transport models seem to be absent from data available now (sec. 2.3.4).

2.3.3 Numerical Representations

For present purposes, rather than employing theoretical spectra for the several components of galactic cosmic rays, we describe the intensities with ad hoc numerical expressions fitted to the data. Such an expression for the integral electron intensity I_e is

$$I_e \approx \frac{2000}{(\alpha E^6+\beta E^3+E^2+\gamma)^{1/4}} + \frac{400}{E^{3/2}} \qquad (11)$$

and its derivative, specifying the differential electron intensity i_e, is

$$i_e \approx \frac{500(6\alpha E^5+3\beta E^2+2E)}{(\alpha E^6+\beta E^3+E^2+\gamma)^{5/4}} + \frac{600}{E^{5/2}} \; . \qquad (12)$$

Here the required units are E in MeV, I_e in $m^{-2}s^{-1}sr^{-1}$, and i_e in $m^{-2}s^{-1}sr^{-1}MeV^{-1}$, and values of $\alpha = 10^{-12}$, $\beta = 10^{-3}$, and $\gamma = 6\times10^4$ allow the observed spectrum (fig. 10) to be fit within 25% for electron energies in the range $1 < E < 3\times10^5$ MeV. To within a factor of 2, the positron intensities are 0.1 times the electron intensities at the same energy.

For the protons, comparable expressions are

$$I_p = \frac{3\times10^5}{[\alpha E^6+\beta E^4+E^2+(1.8)E_2^{\,2}]^{2/5}} + \frac{10^7}{E^{3/5}(E+\gamma E_2^{\,2})} \qquad (13)$$

and

$$i_p = \frac{1.2\times10^5(6\alpha E^5+4\beta E^3+2E)}{[\alpha E^6+\beta E^4+E^2+(1.8)E_2^{\,2}]^{7/5}} + \frac{10^7[(1.6)E+(0.6)\gamma E_2^{\,2}]}{E^{8/5}(E+\gamma E_2^{\,2})^2} . \qquad (14)$$

Here the required units are the same as for electrons, and values of $\alpha = 9\times10^{-29}$, $\beta = 5\times10^{-9}$, and $\gamma = 8$ allow the observed spectra (fig. 7 and 8) to be fit within 50%. Here also E_2 is the energy at which i_p is maximum, and for the best fit to fig. 8 the values 300, 400, and 550 MeV should be assigned to E_2 in 1965, 1967 and 1969 respectively. For the same values of the energy E, specified in MeV/nucleon, the intensities of other nuclear species may be approximated by multiplying the proton expressions by values appropriately chosen from fig. 9 and 10.

2.3.4 Time and Position Dependences

The modulation of the intensities of galactic cosmic rays imposes variations up to an order of magnitude on the low energy ($\lesssim$ 100 MeV) particles on a time scale of a few years (fig. 8). Even though the most plausible explanation involves the interaction of the galactic cosmic rays with interplanetary magnetic fields controlled by the solar wind, quantitative correlations with solar activity indicators are not reliable even over the short time span from 1965 (near solar minimum) to the present (well beyond solar maximum). Thus, as an ad hoc technique for representation of past data and predictions for spacecraft design, values for E_2 (energy parameter in the proton fit, sec. 2.3.3) are suggested as follows:

$$E_2 = \begin{cases} 576 - |64(t-1970)| & \text{for } 1964.75 \le t \le 1975.25 \\ 576 - |64(t-1980.5)| & \text{for } 1975.25 \le t \le 1985.75. \end{cases} \qquad (15)$$

Here E_2 is in MeV, t is the date in years, and a solar cycle of 21 years (half-cycle 10.5 years) has been assumed. This representation for E_2 is shown in fig. 12, and approximately reproduces the E_2 values cited in sec. 2.3.3.

Data for the heliocentric gradient (near the earth) of galactic cosmic ray intensities, as measured by spacecraft experiments, include very diverse (and possibly energy-sensitive) results, suggesting the unreliability of inferences on any heliocentric distance dependence from data with a baseline of only several tenths of an astronomical unit (O'Gallagher, 1972; Webber and Lezniak, 1973). The data having the longest baseline in heliocentric distance are those returned by Pioneer 10, which out to about 4 AU from the sun yield a null result for the variation of intensity (protons above about 80 MeV) with distance (Van Allen, 1973). It has further been demonstrated that, at low energies, theory permits several very different interstellar cosmic ray spectra (Urch and Gleeson, 1972) to match observed ones near the earth after modulation (by convection, diffusion, and other mechanisms). Thus it is difficult to rationally select an interstellar spectrum and a corresponding description for the transition from 1 AU to interstellar space. Thus we adopt here the simplest description consistent with the observations, that in all interplanetary space cosmic ray intensities and their energy spectra are identical to those observed just beyond the earth's magnetosphere. This is equivalent to assuming a modulation region, large compared to the earth's orbit (possibly the heliosphere), within which cosmic ray intensities are uniform in space (but modulated in time), and rather different at low energies from the (presumably time-independent) intensities in interstellar space.

Data on the time and position dependences of the electron component (e.g., Earl, 1972, and Schmidt, 1972) are less thoroughly developed than for the protons, so we adopt the spectra specified by eq. 11 and 12 for all interplanetary times and positions.

3. CRITERIA

Quantitative descriptions for charged particle environments in interplanetary space, including time, position and energy dependences, probabilities and other parameters, are specified in the following sections. They include the solar wind, energetic solar protons and electrons, and galactic cosmic rays, and obtain in the heliocentric distance interval $0.1 < S < 10$ AU. The basic relationships among intensity, flux and fluence are included among the definitions of symbols and terms in Appendices A and B.

3.1 Solar Wind

The solar wind is a fully ionized plasma continuously streaming approximately outward from the sun with variable concentrations, velocities and temperatures of electrons, protons, and heavier positive ions, and entraining magnetic field lines. Table 1 specifies (for several pertinent quantities) average values, ranges, and dependences on heliocentric distance S. The distribution of instantaneous (any time scale $\leq$ a week) values of these quantities is somewhat broader than the interval (between the two values given, suitably modified by the dependence on S) in table 1, and the median, average and most probable values are comparable. Commonly streams of solar wind plasma exist, with high flow speed and temperature associated with low concentration; interactions within and among moving streams include acoustic and plasma waves, shocks, and discontinuities. To estimate cumulative (any time scale $\geq$ a month) effects of solar wind impact, average values are appropriate. For heavier ions in the solar wind, both the flow and thermal speeds match those of the protons, and the concentrations are ≤ 0.2 cm^{-3}, which represents a typical value for He^{++} (the most common ion after H^{+}).

TABLE 1. VALUES NEAR 1 AU AND RADIAL DEPENDENCES FOR SOLAR WIND PARAMETERS

		AVERAGE	RANGE*	RADIAL DEPENDENCE
PROTON	concentration, cm^{-3}	5	7 to 2.5	S^{-2}
	flow speed, km/s	425	350 to 550	none
	thermal speed, km/s	50	35 to 70	$S^{-0.5}$
	temperature, K	8×10^4	$(5 \text{ to } 15)\times10^4$	$S^{-1\pm0.5}$
	energy (flow), eV	900	600 to 1500	none
	flux (flow), $m^{-2}s^{-1}$	2×10^{12}	$(2.5 \text{ to } 1.4)\times10^{12}$	S^{-2}
ELECTRON	concentration, cm^{-3}	5	7 to 2.5	S^{-2}
	flow speed, km/s	425	350 to 550 **	none
	thermal speed, km/s	2700	2100 to 3300	$S^{-0.5}$
	temperature, K	1.5×10^5	$(1 \text{ to } 2)\times10^5$	$S^{-1\pm0.5}$
	energy (thermal), eV	20	13 to 30	$S^{-1\pm0.5}$
	flux (thermal), $m^{-2}s^{-1}$	10^{13}	$(5 \text{ to } 15)\times10^{12}$	$S^{-3\pm0.5}$
MAGNETIC FIELD	strength, nT (gammas)	5	2 to 7	S^{-1}

* Typically data fall within this range most (say 60%) of the time.

** Stream correlated quantities appear above the dashed line (fast stream values at right, slow at left); below it parameters listed are not strongly correlated in streams.

3.2 Solar Particle Events

Solar particle events are sporadic injections of energetic charged particles into interplanetary space, at very irregular intervals (mean frequency of the order of one per month) and depending on solar activity. Within each event, the particle intensity varies markedly with time (from time scales less than a second to a few days for the rise and decay of an entire event), position, direction and energy. These dependences are unpredictable for any given combinations of individual event and detector trajectory, so in the following description only the peak intensity (independent of time, position, and direction), cumulative event fluence, and their average energy spectra are specified on a probabilistic basis.

3.2.1 Peak Proton Intensity

The integral intensity I of protons with kinetic energy $>E$ (in MeV) is on the average proportional to $E^{-1.55}$, is taken to depend on the heliocentric distance S (in AU) as S^{-3} (independent of direction and of heliocentric latitude and longitude), and has a peak during the event (as observed near the earth, at S = 1 AU) of the order of magnitude of $10^6 m^{-2} s^{-1} sr^{-1}$ for $E > 30$ MeV. The mean number of events $N(I)$ in which the intensity exceeds I (in $m^{-2} s^{-1} sr^{-1}$) has been related to the smoothed sunspot number R_z by

$$N(I) = \sum C \exp[-3.69(S^3 I E^{1.55}/1.56\times10^9)^{\gamma_1}] . \quad (16)$$

Here the parameters are specified by

$$C = \text{smaller of } [1.0, (1/6)\exp(R_z/42)] \text{ per month}, \quad (17)$$

$$\gamma_1 = \text{larger of } [(468-R_z)/1450, (R_z-36)/275], \quad (18)$$

and the summation in eq. 16 extends over those months (and/or fractions of months) of interest. The sunspot numbers R_z are specified in *Solar Geophysical Data*, Part I, in table 2, and in fig. 11.

TABLE 2. SMOOTHED SUNSPOT NUMBERS R_z FOR 1970 THROUGH 1989

	JAN	FEB	MAR	APR	MAY	JUN	JULY	AUG	SEPT	OCT	NOV	DEC
1970	105.6	106.0	106.2	106.1	105.8	105.3	103.8	101.0	97.2	93.9	89.4	84.1
1971	80.4	77.8	74.4	70.9	68.1	66.7	65.4	64.6	65.8	66.2	66.8	69.4
1972	70.8	71.2	72.4	73.4	72.9	70.5	68.1	65.4	62.0	62.5	62.0	61.1
1973	60.0	58.3	56.3	54.3	52.7	50.7	49.1	48.2	46.6	44.2	41.8	39.7
1974	38.2	37.0	36.1	35.1	34.4	33.2	31.7	29.8	27.6	25.6	23.6	22.1
1975	20.9	19.3	10.3	5.0	5.0	5.0	5.2	5.5	5.9	6.3	7.2	8.1
1976*	9.4	10.7	12.4	14.2	17.0	19.8	23.3	26.8	30.4	34.1	37.7	41.4
1977	45.4	49.4	53.4	57.4	61.6	65.8	69.4	72.9	75.9	78.8	81.9	84.9
1978	87.5	90.0	92.2	94.3	96.3	98.2	101.0	104.0	107.0	110.0	113.0	116.0
1979	115.0	113.0	111.0	109.0	107.0	105.0	104.6	104.2	103.9	103.6	102.9	102.1
1980	101.3	100.4	99.5	98.5	97.4	96.3	93.0	92.6	91.2	89.8	88.0	86.1
1981	83.9	81.6	79.3	77.0	74.8	72.6	69.9	67.3	65.4	63.6	61.9	60.3
1982	58.6	56.9	55.1	53.3	51.3	49.4	47.8	46.3	44.4	42.6	40.9	39.3
1983	37.8	36.3	35.0	33.7	32.5	31.3	30.1	29.0	27.9	26.8	26.0	25.3
1984	24.6	24.0	23.3	22.6	21.6	20.6	19.6	18.6	17.6	16.6	15.6	14.6
1985	13.6	12.6	11.6	10.6	9.6	8.6	7.6	6.6	6.6	5.0	5.0	5.0
1986*	5.2	5.5	5.9	6.3	7.2	8.1	9.4	10.7	12.4	14.2	17.0	19.8
1987	23.3	26.8	30.4	34.1	37.7	41.4	45.4	49.4	53.4	57.4	61.6	65.8
1988	69.4	72.9	75.9	78.8	81.9	84.9	87.5	90.0	92.2	94.3	96.3	98.2
1989	101.0	104.0	107.0	110.0	113.0	116.0	115.0	113.0	111.0	109.0	107.0	105.0

* These lines represent estimated divisions between adjacent solar cycles. For cycle 20 observed values are used through 1972, and predicted values through 1974. For cycles 21 and 22 the mean of cycle 8-19 is used.

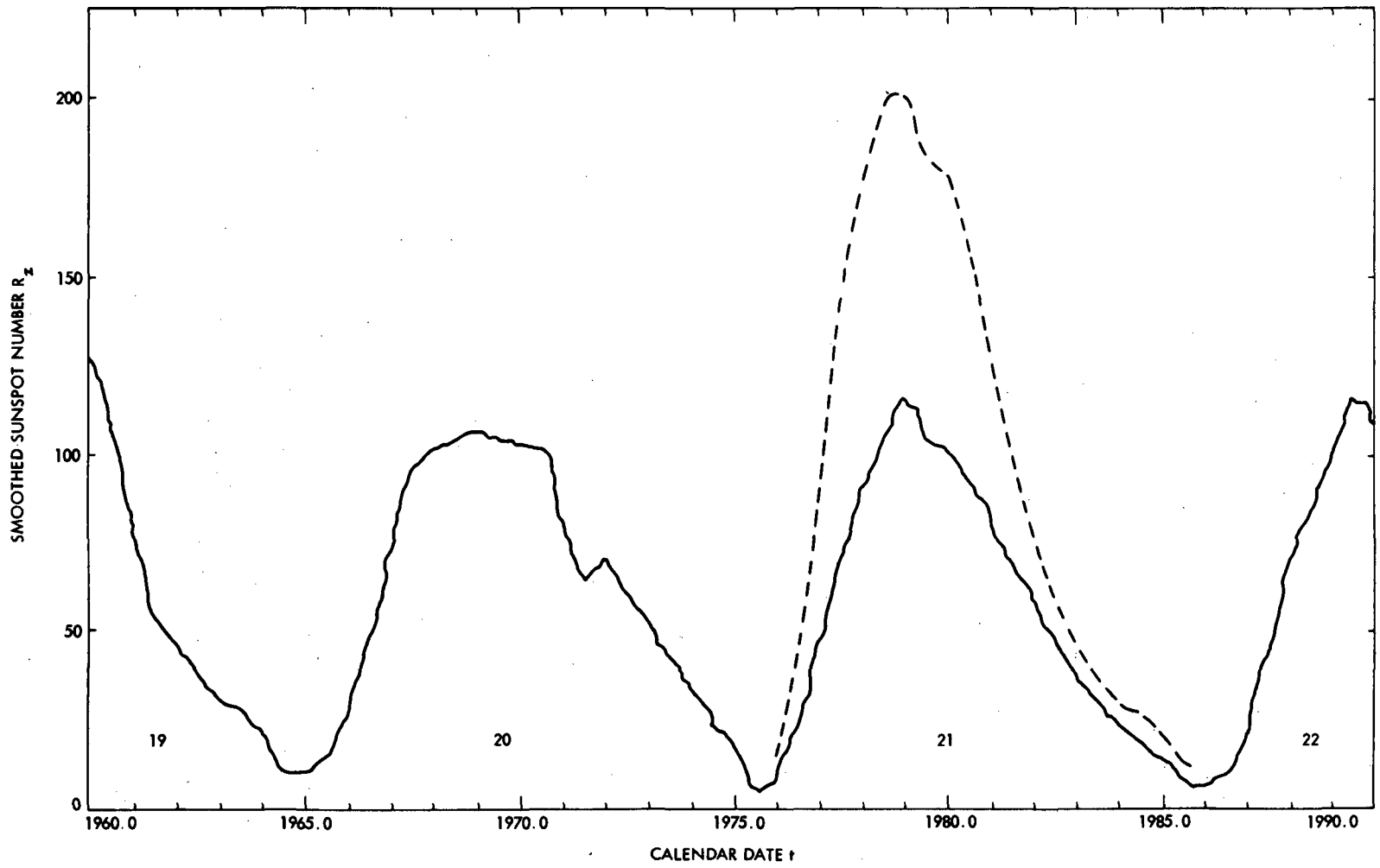

Figure 11. Smoothed sunspot numbers as a function of time. For cycles 19 and 20, observed values are used through 1972, and predicted values through 1974. For cycles 21 and 22 the mean of cycles 8-19 is used, and data for cycle 19 is shown (dashed line) as representative of 95 percentile values.

The probability that the peak intensity will exceed I at least once during an interval is specified by

$$P(I) = 1 - exp[-N(I)] . \tag{19}$$

The omnidirectional flux in $m^{-2}s^{-1}$ is given by $J = 4\pi I$. A computer program has been written to evaluate eq. 16 and 19.

3.2.2 Proton Fluence

The cumulative integral fluence F of protons with kinetic energy $> E$ (in MeV) is on the average proportional to $E^{-1.87}$, is taken to depend on the heliocentric distance S (in AU) as S^{-2} (independent of direction and of heliocentric latitude and longitude), and has values for an event (as observed near the earth, at $S = 1$ AU) of the order of magnitude of $10^{12}m^{-2}$ for $E > 30$ MeV. The mean number of events $N(F)$ for which the fluence exceeds F (in m^{-2}) has been related to the smoothed sunspot number R_z by

$$N(F) = \sum C \; exp[-3.85(S^2 F E^{1.87}/6.94\times10^{15})^{\gamma_2}]. \tag{20}$$

Here the parameters are specified by eq. 17, by

$$\gamma_2 = \text{larger of } [(289-R_z)/819, (R_z-50)/243] , \tag{21}$$

and the summation in eq. 20 extends over those months (and/or fractions of months) of interest. The sunspot number R_z are specified in *Solar Geophysical Data*, Part I, in table 2, and in fig. 11.

The probability that the fluence accumulated over one or more events will exceed F is specified by the sum

$$P(F) = \sum_{\ell=1}^{\infty} \left\{ 1 - [e^{-N_o}] \sum_{k=1}^{\ell-1} N_o{}^k/k! \right\} D_\ell(F) \tag{22}$$

Here

$$N_o = N(F) \text{ evaluated at } F = 0, \tag{23}$$

$$D_1(F) = N(F)/N_o, \tag{24}$$

$$D_\ell(F) = N_o^{-1} \int_0^F [\, -dN(x)/dx] D_{\ell-1}(F-x)\, dx \tag{25}$$

and a number of terms $\ell \leq (N_o + 20)$ is usually sufficient to evaluate $P(F)$ to about 10^{-4}. A computer program has been written to evaluate eq. 20 and 22 through 25.

3.2.3 Other Particles and Energies

The above proton description serves in the energy range $10 \leq E \leq 10^3$ MeV, above which galactic cosmic ray protons (sec. 3.3) dominate. In the interval between solar wind energies (1 keV) and 10 MeV, expressions which approximate the peak solar proton integral intensity in the form $I = (10^8 \text{m}^{-2}\text{s}^{-1}\text{sr}^{-1})/S^3E^{1.2}$ and (in place of fluence) the average solar proton integral intensity $I = (10^6 \text{m}^{-2}\text{s}^{-1}\text{sr}^{-1})/S^2E^{1.7}$ are appropriate for heliocentric distance S in AU and proton kinetic energy E in MeV for $10^{-3} < E < 10$ MeV. At all energies helium nuclei intensities are of the order of 0,05 times the proton intensities, and other positive ions may be neglected.

For solar particle event electrons, expressions which approximate the peak electron integral intensity $I = (10^5 \text{m}^{-2}\text{s}^{-1}\text{sr}^{-1})/S^3E^2$ and (in place of fluence) the average electron integral intensity $I = (400\ \text{m}^{-2}\text{s}^{-1}\text{sr}^{-1})/S^2E^2$ are appropriate for heliocentric distance S in AU and electron kinetic energy E in MeV for $2\times10^5 < E < 10$ MeV. Beyond this range the solar wind or galactic cosmic ray electron descriptions pertain.

3.3 Galactic Cosmic Rays

Galactic cosmic rays are relativistic charged particles (predominantly protons, with some electrons, positrons, and heavy nuclei) continuously present in interplanetary space at integral fluxes $\lesssim 3\times10^{4}\,m^{-2}s^{-1}$ and energies extending indefinitely upward from below 100 MeV. The integral and differential intensities of the electrons as functions of electron kinetic energy E are represented to within 25% by

$$I_e = \frac{2000}{(\alpha E^6+\beta E^3+E^2+\gamma)^{1/4}} + \frac{400}{E^{3/2}} \tag{26}$$

and

$$i_e = \frac{500(6\alpha E^5+3\beta E^2+2E)}{(\alpha E^6+\beta E^3+E^2+\gamma)^{5/4}} + \frac{600}{E^{5/2}} . \tag{27}$$

Here the required units are E in MeV (for $1 < E < 3\times10^{5}$ MeV), I_e in $m^{-2}s^{-1}sr^{-1}$, and i_e in $m^{-2}s^{-1}sr^{-1}MeV^{-1}$, and the parameter values are $\alpha = 10^{-12}$, $\beta = 10^{-3}$, and $\gamma = 6\times10^{4}$. For a precision of about 10^{-2}, terms proportional to α may be ignored for $E < 250$ MeV, and the last of the terms in the sum for I_e or i_e may be ignored for $E > 250$ MeV. The positron intensities are $0.1\times2^{\pm1}$ times the electron intensities (eq. 26 and 27) at the same energy.

The integral and differential intensities of the protons as functions of proton kinetic energy E are represented to within 50% by

$$I_p = \frac{3\times10^{5}}{[\alpha E^6+\beta E^4+E^2+(1.8)E_2^{\,2}]^{2/5}} + \frac{10^{7}}{E^{3/5}(E+\gamma E_2^{\,2})} \tag{28}$$

and

$$i_p = \frac{1.2\times10^{5}(6\alpha E^5+4\beta E^3+2E)}{[\alpha E^6+\beta E^4+E^2+(1.8)E_2^{\,2}]^{7/5}} + \frac{10^{7}[(1.6)E+0.6\gamma E_2^{\,2}]}{E^{8/5}(E+\gamma E_2^{\,2})^2} . \tag{29}$$

Here the required units are the same as for electrons, and the parameter values are $\alpha = 9\times10^{-29}$, $\beta = 5\times10^{-9}$, and $\gamma = 8$. For a precision of about 10^{-2}, terms proportional to α may be ignored for $E < 10^{9}$ MeV, terms proportional to β may be ignored for $E < 2000$ MeV, and the last of the two terms in the sum for I_p

or i_p may be ignored for $80 < E < 10^{10}$ MeV. The energy parameter E_2 represents the location of a maximum in the proton differential intensity i_p and is variable in the solar cycle. Suitable values are shown in fig. 12 (cf. also fig. 11) and are given by

$$E_2 = \begin{cases} 576 - |64(t-1970)| & \text{for } 1964.75 \le t \le 1975.25 \\ 576 - |64(t-1980.5)| & \text{for } 1975.25 \le t \le 1985.75 \end{cases} \tag{30}$$

where t represents the date in solar cycle 20 or 21.

For the same values of kinetic energy E, specified in MeV/nucleon, the intensities of other cosmic ray nuclei are related to the proton intensities (eq. 28 and 29) by the factors specified in table 3.

With the exception of the time variations of E_2 (eq. 28 through 30), all the intensities are taken independent of time, direction, and position in interplanetary space. The numerical representations (eq. 26 through 29) for the integral and differential intensities are shown in fig. 13.

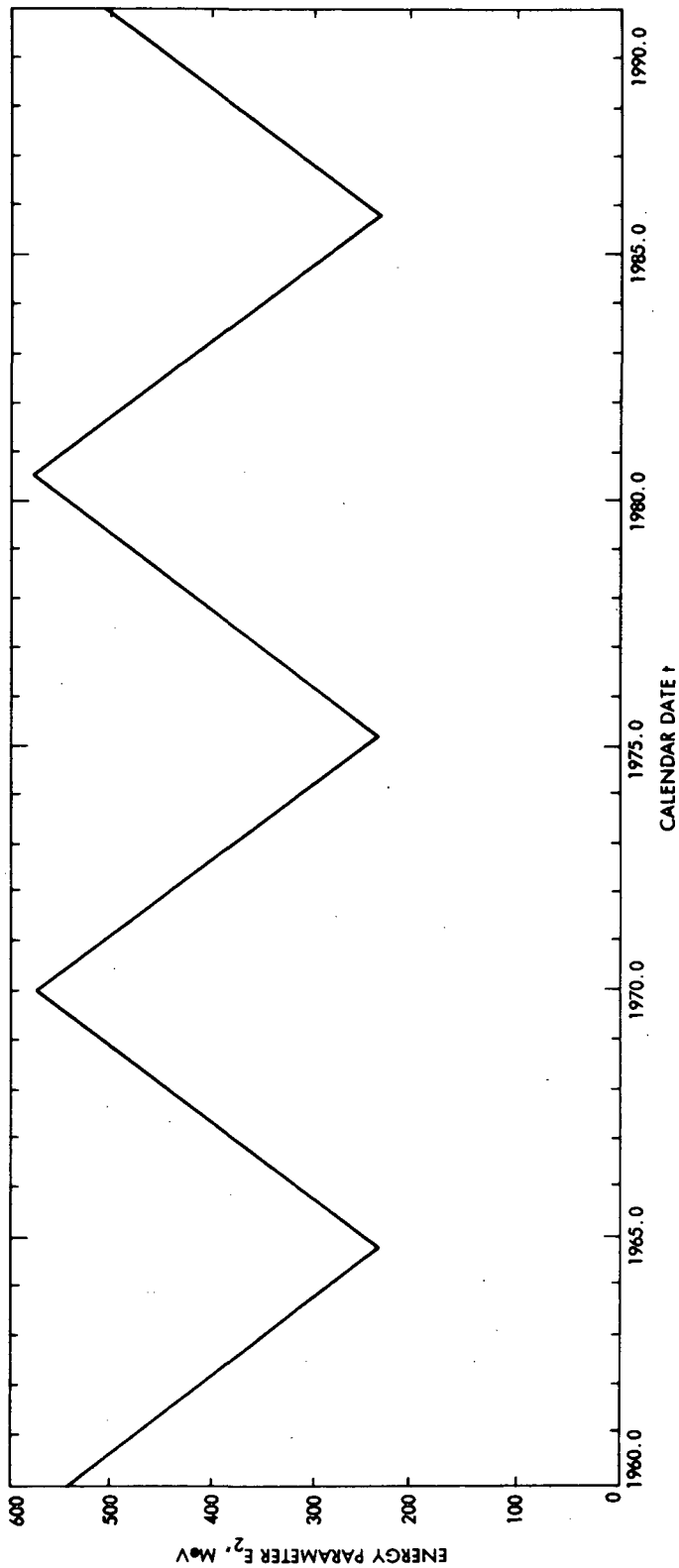

Figure 12. Time-dependence of the energy parameter E_2 for the numerical representation of galactic cosmic ray proton intensities modulated by solar activity.

TABLE 3. INTENSITY RATIOS (TO PROTONS) FOR THE TWELVE MOST ABUNDANT COSMIC RAY NUCLEI

NUCLEUS	ATOMIC NUMBER (CHARGE)	ATOMIC WEIGHT (# NUCLEONS)	RATIO TO PROTONS *
H	1	1	1.0
He	2	4	0.1
Li	3	7	4×10^{-4}
Be	4	9	2.5×10^{-4}
B	5	11	6×10^{-4}
C	6	12	2.5×10^{-3}
N	7	14	6×10^{-4}
O	8	16	2.5×10^{-3}
Ne	10	20	4×10^{-4}
Mg	12	24	4×10^{-4}
Si	14	28	3×10^{-4}
Fe	26	56	2.5×10^{-4}

* Accuracy in most cases better than about 50%

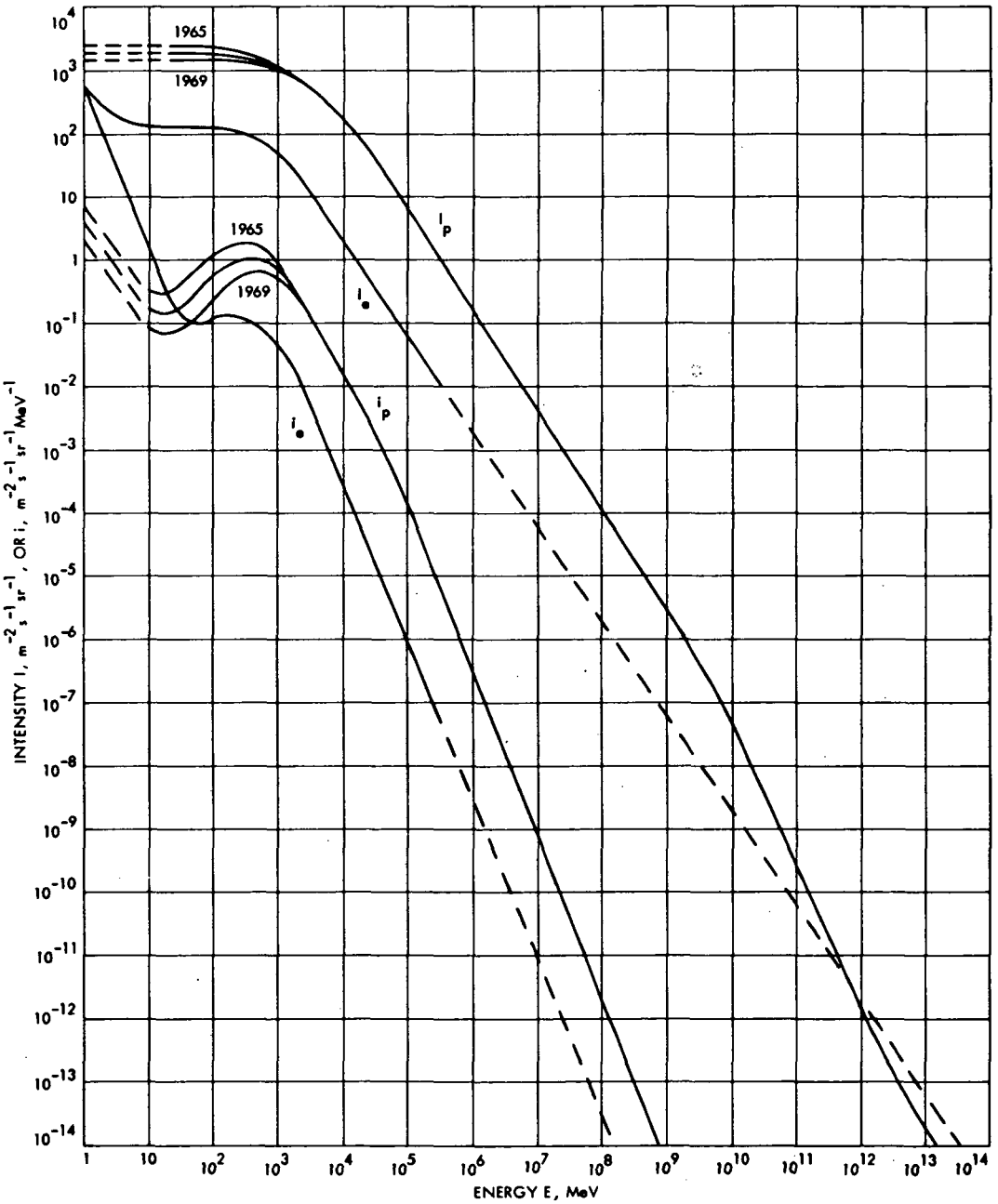

Figure 13. Intensity spectra of galactic cosmic ray electrons and protons. Solid portions represent data and dashed portions extrapolations. The three branches of the proton curves represent the effect of modulation in 1965, 1967, and 1969.

Page Intentionally Left Blank

APPENDIX A. SYMBOLS*

A	anisotropy
C	rate coefficient for solar particle events ($month^{-1}$)
$D_\ell(F)$	dummy function for proton probability calculation
E	charged particle kinetic energy (MeV)
E_2	energy parameter for galactic cosmic ray protons (MeV)
f	differential **fluence** (m^{-2} MeV^{-1})
F	integral **fluence** (m^{-2})
i	differential **intensity** ($m^{-2}s^{-1}sr^{-1}MeV^{-1}$)
I	integral **intensity** ($m^{-2}s^{-1}sr^{-1}$)
j	differential (omnidirectional) **flux** ($m^{-2}s^{-1}$ MeV^{-1})
J	integral (omnidirectional) **flux** ($m^{-2}s^{-1}$)
N_o	mean number of solar proton events
$N(F)$	mean number of solar proton events exceeding **fluence** F
$N(I)$	mean number of solar proton events exceeding **intensity** I
$P(F)$	probability that mission **fluence** exceeds F
$P(I)$	probability that mission peak **intensity** exceeds I
$P_k(F)$	$P(F)$ if exactly k events occur
R_z	monthly smoothed Zürich sunspot number
S	heliocentric distance (AU)
t	time (calendar years)
α, β, γ	parameters in numerical representations of galactic cosmic ray **intensity**
γ_1	peak **intensity** exponent for solar protons
γ_2	**fluence** exponent for solar protons

* Words in **bold face** are defined in the Glossary (Appendix B).

APPENDIX B. GLOSSARY*

anisotropy (A) The anisotropy is a dimensionless measure of the sensitivity of the local particle distribution (or intensity) to direction (of incidence). There are diverse formal definitions, in all of which $A = 0$ when the distribution is isotropic (independent of direction); otherwise, for $A>0$, sample usage includes $A = (I_{max} - I_{min})/I_{max}$ where I_{max} and I_{min} are **intensities** in the directions of maximum and minimum **intensity**, or $A = (T_\perp - T_\parallel)/T_\parallel$ where $T_\perp$ and $T_\parallel$ are temperatures perpendicular and parallel to the local magnetic field.

fluence (f or F) The fluence is the number of particles entering a unit area in a finite time. Like **intensity** (the basic quantity), it is differential (f) or integral (F). Thus $f = \int j\, dt = \int\int i\, d\Omega\, dt = -\, dF/dE$ and $F = \int J\, dt = \int_E^\infty dE \int\int i\, d\Omega\, dt = \int_E^\infty f\, dE$. Units for f are $m^{-2}MeV^{-1}$ and for F are m^{-2}.

* Cross references within the Glossary are indicated by **bold face**.

flux (j or J) The omnidirectional flux is the number of particles entering a unit area per unit time. Like **intensity** (the basic quantity), it is differential (j) or integral (J). Thus $j = \int i \, d\Omega = - dJ/dE$ and $J = \int I \, d\Omega = \int_E^\infty dE \int i \, d\Omega = \int_E^\infty j \, dE$. In the isotropic ($A$=0) case, $j = 4\pi i$ and $J = 4\pi I$. Units for j are $m^{-2}s^{-1}MeV^{-1}$ and for J are $m^{-2}s^{-1}$.

intensity (i or I) The intensity is the number of particles crossing a unit area, per unit time, from within a unit solid angle. It may depend on direction as well as on time and position, and is either differential (i, per unit energy interval) or integral (I, for energies $>E$), in both cases depending on particle kinetic energy E. Thus $i = - dI/dE$ and $I = \int_E^\infty i \, dE$. Units for i are $m^{-2}s^{-1}sr^{-1}MeV^{-1}$ and for I are $m^{-2}s^{-1}sr^{-1}$.

APPENDIX C. Solar Particle Fluence Probabilities

This appendix derives expressions for the probability $P(F)$ that the fluence exceeds F when the mean number of events in which the event fluence exceeds F is given by $N(F)$. If the distribution is Poisson, then the probability that exactly k events occur is $e^{-N_o}(N_o)^k/k!$. Consider the probability $P_k(F)$ that, if exactly k events do occur, the fluence exceeds F. Clearly for the cases $k = 0$ (no events) and $k = 1$ (one event) we can set $P_o(F) = 0$ and $P_1(F) = N(F)/N_o$ respectively. To construct $P_2(F)$, we add, to the probability $P_1(F)$ that F or more fluence was accumulated in the first event, the probability that the second event (with the same probability distribution as the first) adds enough to the fluence f from the first event to total F or more, as given by

$$P_2(F) = P_1(F) + \int_0^F [-dP_1(f)/df]P_1(F-f)\,df \; . \tag{C-1}$$

A similar argument holds for each successive event, resulting in a form which can be integrated by parts as follows for $k \geq 2$:

$$\begin{aligned} P_k(F) &= P_{k-1}(F) + \int_0^F [-dP_{k-1}(f)/df]P_1(F-f)\,df \\ &= P_{k-1}(F) - P_{k-1} + P_1(F) + \int_0^F P_{k-1}(f)[dP_1(F-f)/df]\,df \\ &= P_1(F) + \int_0^F [-dP_1(x)/dx]P_{k-1}(F-x)\,dx \\ &= N(F)/N_o + N_o^{-1}\int_0^F [-dN(x)/dx)]P_{k-1}(F-x)\,dx \; . \end{aligned} \tag{C-2}$$

If we define $D_\ell(F)$ by $D_1(F) = P_1(F) = N(F)/N_o$ and, for $\ell \geq 2$ by $D_\ell(F) = P_\ell(F) - P_{\ell-1}(F)$ we see that

$$D_2(F) = N_o^{-2}\int_0^F [-dN(x)/dx][N(F-x)]\,dx \tag{C-3}$$

and that for $\ell \geq 3$

$$D_\ell(F) = N_o^{-1} \int_0^F [-\, dN(x)/dx][P_{\ell-1}(F-x) - P_{\ell-2}(F-x)]\, dx$$

$$= N_o^{-1} \int_0^F [-\, dN(x)/dx]\, D_{\ell-1}(F-x)\, dx \ . \qquad \text{(C-4)}$$

The definition of $D_\ell(F)$ also leads to

$$P_k(F) = \sum_{\ell=1}^{k} D_\ell(F) \ . \qquad \text{(C-5)}$$

We now use the Poisson distribution, the definitions of $P_k(F)$ and $D_\ell(F)$, the relations just derived, an exchange of the order of summation, and the series expansion for $exp(N_o)$ to derive the total probability $P(F)$ that the fluence exceeds F in the form

$$P(F) = \sum_{k=1}^{\infty} [e^{-N_o}\ (N_o)^k/k!\,]\ P_k(F)$$

$$= e^{-N_o} \sum_{k=1}^{\infty} [(N_o)^k/k!\ ] \sum_{\ell=1}^{k} D_\ell(F)$$

$$= e^{-N_o} \sum_{\ell=1}^{\infty} D_\ell(F) \sum_{k=\ell}^{\infty} (N_o)^k/k!$$

$$= \sum_{\ell=1}^{\infty} D_\ell(F)\ e^{-N_o}\ [e^{N_o} - \sum_{k=0}^{\ell-1} (N_o)^k/k!\ ]$$

$$= \sum_{\ell=1}^{\infty} D_\ell(F)\ [\ 1 - e^{-N_o} \sum_{k=0}^{\ell-1} (N_o)^k/k!\ ] \qquad \text{(C-6)}$$

Here the last series requires fewer terms than the first for the same relative accuracy. The last four equations (7 through 10) of sec. 2.2.5 have now been derived.

REFERENCES

Atwell, W., 1972: "The Significant Solar Proton Events in the 20th Solar Cycle for the Period October 1964 to March 1970", NASA TM X-2440, pp. 329-335.

Axford, W. I., 1968: "Observations of the Interplanetary Plasma", *Space Sci. Revs.* Vol. 8, No. 3, pp. 331-365.

Axford, W. I., 1972: "Interaction of the Solar Wind with the Interstellar Medium", NASA SP-308, pp. 609-660.

Bame, S. J., J. R. Asbridge, A. J. Hundhausen, and M. D. Montgomery, 1970: "Solar Wind Ions: $^{56}Fe^{+8}$ to $^{56}Fe^{+12}$, $^{28}Si^{+7}$, $^{28}Si^{+8}$, $^{28}Si^{+9}$, and $^{16}O^{+6}$", *J. Geophys. Res.* Vol. 75, No. 31, pp. 6360-6365.

Bame, S. J., 1972: "Spacecraft Observations of the Solar Wind Composition", NASA SP-308, pp. 535-558.

Bhatnagar, V. P., and H. J. Fahr, 1972: "Solar Wind Expansion Beyond the Heliosphere", *Planet. Space Sci.* Vol. 20, No. 4, pp. 445-460.

Brandt, J. C., 1967: "Interplanetary Gas XIII. Gross Plasma Velocities from the Orientations of Ionic Comet Tails", *Astrophys. J.* Vol. 147, No. 1, pp. 201-219.

Brandt, J. C., 1970: *Introduction to the Solar Wind,* Freeman, San Francisco, 199 pp.

Burlaga, L. F., 1972: "Microstructure of the Interplanetary Medium", NASA SP-308, pp. 309-332.

Burrell, M. O., 1972: "The Risk of Solar Proton Events to Space Missions", NASA TM X-2440, pp. 310-323.

Cline, T. L., and F. B. McDonald, 1968: "Relativistic Electrons from Solar Flares", *Solar Physics* Vol. 5, No. 4, pp. 507-530.

Cohen, M. H., E. J. Gundermann, H. E. Hardebeck, and L. E. Sharp, 1967: "Interplanetary Scintillations II. Observations", *Astrophys. J.* Vol. 147, No. 2, pp. 449-466.

Cuperman, S., A. Harten, and M. Dryer, 1972: "Characteristics of the Quiet Solar Wind Beyond the Earth's Orbit", *Astrophys. J.* Vol. 177, No. 2, pp. 555-566.

Davis, L., Jr., 1972: "The Interplanetary Magnetic Field", NASA SP-308, pp. 93-114.

Dietrich, W. F., 1973: "The Differential Energy Spectra of Solar-Flare ^{1}H, ^{3}He, and ^{4}He", *Astrophys. J.* Vol. 180, No. 3, pp. 955-973.

Dollman, T. S., and A. T. Bechtelheimer, 1967: "Construction of Probability Envelopes of Flux-Energy Spectrum for Solar Proton Events", NASA TM X-53647, pp. 110-113.

Earl, J. A., 1972: "Modulation of Cosmic-Ray Electrons", *Astrophys. J.* Vol. 178, No. 3, pp. 857-862.

Englade, R. C., 1971: "A Computational Model for Solar Flare Particle Propagation", *J. Geophys. Res.* Vol. 76, No. 4, pp. 768-791.

Fichtel, C. E., and D. V. Reames, 1968: "Cosmic-Ray Propagation", *Phys. Rev.* Vol. 175, No. 5, pp. 1564-1576.

Gonzalez, C. C., and E. L. Divita, 1968: "Solar Proton Forecast System and Procedures Used During the Mariner V Mission", JPL TR 32-1303, 35 pp.

Haffner, J. W., 1972: "Time Behavior of Solar Flare Particles to 5 AU", NASA TM X-2440, pp. 336-344.

Hewish, A., and M. D. Symonds, 1969: "Radio Investigation of the Solar Plasma", *Planet. Space Sci.* Vol. 17, pp. 313-320.

Hsieh, K. C., G. M. Mason, and J. A. Simpson, 1971: "Cosmic-Ray ^{2}H from Satellite Measurements, 1965-1969", *Astrophys. J.* Vol. 166, No. 1, pp. 221-233.

Hundhausen, A. J., S. J. Bame, J. R. Asbridge, and S. J. Sydoriak, 1970: "Solar Wind Proton Properties: Vela 3 Observations from July 1965 to June 1967", *J. Geophys. Res.* Vol. 75, No. 25, pp. 4643-4657.

Jokipii, J. R., 1971: "Propagation of Cosmic Rays in the Solar Wind", *Revs. Geophys. Space Phys.* Vol. 9, No. 1, pp. 27-87.

Lin, R. P., and K. A. Anderson, 1967: "Electrons > 40 keV and Protons > 500 keV of Solar Origin", *Solar Physics* Vol. 1, No. 3/4, pp. 446-464.

McCracken, K. C., U. R. Rao, and N. F. Ness, 1968: "Interrelationship of Cosmic-Ray Anisotropies and the Interplanetary Magnetic Field", *J. Geophys. Res.* Vol. 73, No. 13, pp. 4159-4166.

McDonald, F. B., 1963: *Solar Proton Manual,* NASA TR R-169, 117 pp.

McDonald, F. B., T. L. Cline, and G. M. Simnett, 1972: "Multifarious Temporal Variations of Low-Energy Relativistic Cosmic-Ray Electrons", *J. Geophys. Res.* Vol. 77, No. 13, pp. 2213-2231.

Montgomery, M. D., 1972: "Average Thermal Characteristics of Solar Wind Electrons", NASA SP-308, pp. 208-218.

Ness, N. F., A. J. Hundhausen, and S. J. Bame, 1971: "Observations of the Interplanetary Medium: Vela 3 and IMP 3, 1965-1967", *J. Geophys. Res.* Vol. 76, No. 28, pp. 6643-6660.

Neugebauer, M., and C. W. Snyder, 1966: "Mariner 2 Observations of the Solar Wind, 1. Average Properties", *J. Geophys. Res.* Vol. 71, No. 19, pp. 4469-4484.

O'Gallagher, J. J., 1972: "Observations of the Radial Gradient of Galactic Cosmic Radiation over a Solar Cycle", *Revs. Geophys. Space Phys.* Vol. 10, No. 3, pp. 821-835.

Parker, E. N., 1958: "Dynamics of the Interplanetary Gas and Magnetic Fields", *Astrophys. J.* Vol. 123, pp. 664-675.

Roberts, W. T. 1966: "Probabilities of Solar Flare Occurrence", NASA TM X-53463, 12 pp.

Schmidt, P. J., 1972: "Cosmic-Ray Electron Spectrum and Its Modulation near Solar Maximum", *J. Geophys. Res.* Vol. 77, No. 19, pp. 3295-3310.

Simpson, J. A., 1971: "Galactic Sources and the Propagation of Cosmic Rays", paper presented that the 12th International Conference on Cosmic Rays, Hobart, Tasmania.

Sreenkantan, B. V., 1972: "Primaries of Extensive Air Showers of Cosmic Radiation", *Space Sci. Revs.* Vol. 14, No. 1, pp. 103-174.

Thomas, J. R., 1972: "Mariner Venus-Mercury 1973 Mission Solar Proton Environment: Fluence and Dose", JPL *QTR* Vol. 2, No. 1, pp. 12-28.

Urch, I. H., and L. J. Gleeson, 1972: "Radial Gradients and Anisotropies due to Galactic Cosmic Rays", *Astrophys. Space Sci.* Vol. 16, No. 1, pp. 55-74.

Van Allen, J. A., 1973: "Heliocentric Radial Dependence of Galactic Cosmic Ray Intensity to and Beyond 3.0 A.U.", AGU *Transactions EOS* Vol. 54, No. 4, p. 407.

Webb, S., and J. J. Quenby, 1973: "Numerical Studies of the Transport of Solar Protons in Interplanetary Space", *Planet. Space Sci.* Vol. 21, No. 1, pp. 23-42.

Webber, W. R., 1963: "An Evaluation of the Radiation Hazard due to Solar Particle Events", Report D2-90469, Boeing, Seattle, 109 pp.

Webber, W. R., and J. A. Lezniak, 1973: "Interplanetary Radial Gradients of Galactic Cosmic Ray Protons and Helium Nuclei: Pioneer 8 and 9 Measurements from 0.75 to 1.10 AU", *J. Geophys. Res.* Vol. 78, No. 13, pp. 1979-2000.

Weddell, J. B., and J. W. Haffner, 1966: "Statistical Evaluation of Proton Radiation from Solar Flares", Report SID 66-421, North American Aviation, Downey, 178 pp.

Wilson, J. W., 1971: "Solar Radiation Hazard for Mars Orbiter", private communication.

Wolfe, J. H., 1972: "Large Scale Structure of the Solar Wind", NASA SP-308, pp. 170-201.

Yucker, W. B., 1972: "Solar Cosmic Ray Hazard to Interplanetary and Earth-Orbital Space Travel", NASA TM X-2440, pp. 345-355.

Anon., 1971: *Solar Electromagnetic Radiation,* NASA SP-8005 (Revised), 33 pp.

Anon., 1971: *The Planet Jupiter (1970)*, NASA SP-8069, 90 pp.

Anon., 1972: *The Planet Saturn (1970),* NASA SP-8091, 99 pp.

Anon., 1972: *The Planets Uranus, Neptune, and Pluto (1971),* NASA SP-8103, 94 pp.

NASA — JPL — Coml., L.A., Calif.